博士論文

Studies on the molecular mechanisms that regulate lifespan in budding yeast

出芽酵母の寿命を制御する分子機構の研究

益村　晃司

広島大学大学院統合生命科学研究科

2023 年 3 月

目次

1. 主論文

Studies on the molecular mechanisms that regulate lifespan in budding yeast
（出芽酵母の寿命を制御する分子機構の研究）
益村 晃司

2. 参考論文

(1) *SKO1* deficiency extends chronological lifespan in *Saccharomyces cerevisiae*,
Koji Masumura, Sachi Matsukami, Kumiko Yonekita, Muneyoshi Kanai,
Kazunori Kume, Dai Hirata, Masaki Mizunuma,
Bioscience, Biotechnology, and Biochemistry, 83(8), 1473-1476 (2019).

(2) *S*-adenosyl-L-homocysteine extends lifespan through methionine restriction effects,
[†] Takafumi Ogawa, [†] Koji Masumura, Yuki Kohara, Muneyoshi Kanai,
Tomoyoshi Soga, Yoshikazu Ohya, T. Keith Blackwell, Masaki Mizunuma,
Aging Cell, 21(5), e13604 (2022).
[†] Takafumi Ogawa and Koji Masumura contributed equally to this work.

3. 関連論文

(1) 酵母のメチオニン代謝系による寿命制御機構
益村 晃司、水沼 正樹
月刊「細胞」、52 巻、11 号、58-61 頁、2020 年

主論文

Contents

General introduction 1

Chapter 1: *SKO1* deficiency extends chronological lifespan in *Saccharomyces cerevisiae* 7

1.1 Introduction 7

1.2 Material and Methods 8

1.3 Results 10

1.4 Discussion 13

Chapter 2: *S*-adenosyl-L-homocysteine extends lifespan through methionine restriction effects methionine restriction 20

2.1 Introduction 20

2.2 Material and Methods 21

2.3 Results 27

2.4 Discussion 30

General conclusions 44

Acknowledgments 48

References 50

General introduction

According to the 2021 statistics, the average life expectancy in Japan has increased for approximately 10 years in the last half century (81.47 and 87.57 years for men and women, respectively). However, the percentage of the population aged 65 years or older is approximately 30%, because of which the population is called a “super aging society.” Consequently, slow economic growth and burden on social security and healthcare are serious dilemmas faced by Japan. Moreover, the health span, i.e., the length of the time for which a person can stay healthy, is 73 and 76 years for men and women, respectively, which implies that individuals suffer from some kind of disorder for approximately 10 years, leading to a decline in their quality of life. Therefore, increasing healthy life expectancy has become an urgent issue in Japan.

Elucidation of the mechanisms of aging and lifespan is one of the most important issues for understanding the extended human healthspan and lifespan. Research on aging and lifespan is expected to provide insights not only to the understanding of biological aging but also the pathogenesis and treatment of various diseases such as cancer, cardiovascular disorders, and neurodegenerative diseases associated with aging. So far, common molecules and mechanisms involved in lifespan regulation have been identified in yeasts, nematodes, flies, mice, and other organisms that can be used as models for humans (Kenyon, 2010). For instance, dietary restrictions (Mair and Dillin, 2008; Sutphin and Kaeberlein, 2008; Fontana *et al*., 2010) such as calorie restriction (CR) and methionine restriction (MetR) (Orentreich *et al*., 1993; Miller *et al*., 2005; Wu *et al*., 2013), inactivation of the mechanistic target of rapamycin complex Ⅰ (mTORC1) pathway (Wullschleger *et al*., 2013), and activation of adenosine monophosphate-

activated protein kinase (AMPK) (Hedbacker and Carlson, 2008) have been reported to extend the lifespan of many organisms. Particularly, the mechanism of CR to extend lifespan was first revealed in yeast, and the sirtuin gene Sir2, an NAD^+-dependent histone deacetylase, was identified as a key player in CR (Imai *et al*., 2000). Furthermore, a search for compounds that induce longevity has been conducted using yeast, and resveratrol, a type of polyphenol, was discovered as a compound that activates Sir2 (Howitz *et al*., 2003). Interestingly, resveratrol extended the lifespan of yeasts, nematodes, and flies without CR (Wood *et al.*, 2004). Thus, although several signaling pathways and molecular mechanisms were involved in the regulation of lifespan, the detailed molecular mechanisms of and the relationship between lifespan and signaling pathways remain unclear.

The budding yeast *Saccharomyces cerevisiae* is a single-cell model organism, and the mechanisms that regulate its fundamental life processes are similar to those of higher organisms. The concept of lifespan also exists in the yeast and the yeast has two lifespan models, namely, the replicative lifespan (RLS), which is the number of divisions in the lifetime of a single mother cell, and the chronological lifespan (CLS), which is the period during which a cell can survive under limited nutritional conditions after it stops dividing after the stationary phase (Mortimer and Johnston, 1959; Fabrizio and Longo, 2003). Since RLS is the number of daughter cells that a mother cell can produce before aging, it provides a model of aging for regularly dividing cells, such as human fibroblasts and cells of the blood cell lineage. In addition, since the regulatory mechanisms of CLS are similar to those of aging in higher organisms, the insights gained from the said mechanisms are vital to understand human aging. The advantage of using yeast for lifespan analysis is that it is easier to obtain data owing to its shorter lifespan compared

to other model organisms. In addition, yeast is easy to analyze genetically and at the molecular level and is cost-efficient. Therefore, yeast is an ideal tool to study the lifespan owing to its various molecular mechanisms and signaling pathways related to lifespan (Botstein and Fink, 2011).

The calcium ion (Ca^{2+}), as a universal intracellular signaling medium, regulates diverse biological processes, such as fertilization, development, cell proliferation, hormone secretion, and memory (Aramburu *et al*., 2000). Previously, Mizunuma *et al*. (1998) analyzed the physiological functions of Ca^{2+} signaling and discovered calcineurin, a Ca^{2+}-dependent serine/threonine phosphatase in budding yeast. Afterward, it was found that Ca^{2+} signaling pathways inhibit the onset of mitosis through the activation of Swe1, a negative regulator of the G2/M phase, via activation of calcineurin and Mpk1, an MAP kinase.

To obtain novel regulators of the cell cycle via Ca^{2+} signaling, Mizunuma *et al*. (2001) screened for suppressers of the sensitivity of $CaCl_2$ exhibited by strains deleted for the cell cycle regulator of *ZDS1*. The *zds1*Δ cells exhibited calcium sensitivity, abnormal polar bud growth, and delayed G2 phase. As a result, *scz1–14* mutations were obtained from *zds1*Δ cells. Interestingly, *scz14* was allelic to the *SIR3* locus involved in aging. The *SIR3* prolongs the RLS of budding yeast, suggesting a link between the *scz* mutant strain and lifespan. Furthermore, Tsubakiyama *et al*. (2011), using the *zds1*Δ strain with shortened RLS, found that calcineurin activation was associated with shortened RLS in the *zds1*Δ strain. These findings suggest that Ca^{2+} homeostasis regulates lifespan. Among *scz* mutants, *sah1/scz7* is a mutant of the *S*-adenosylhomocysteine (SAH) hydrolase *SAH1* (Mizunuma *et al*., 2004). In the *sah1* mutants, the cellular accumulation of SAH, a substrate of *SAH1*, was accompanied by remarkable accumulation of *S*-

adenosyl-L-methionine (SAM). SAM is synthesized from methionine (Met) and ATP using SAM synthetase and is utilized in the majority of biological methylation reactions (Thomas and Surdin-Kerjan, 1997). On demethylation, SAM is converted into SAH, a potent competitive inhibitor of SAM-dependent methyltransferases. Therefore, *SAH1*, encoding SAH hydrolase, is an essential gene for cell growth. Indeed, the *sah1* mutants exhibited a high accumulation of SAH and impaired proliferation, suggesting a link between Met metabolism and lifespan. Moreover, Ogawa *et al*. (2016) measured the lifespan of *sah1* mutants and found that they had shorter CLS and RLS than wild-type (WT) cells. Therefore, to obtain novel regulators of lifespan extension, we screened for mutants that inhibit growth retardation of *sah1* mutants and obtained 116 suppressor mutants. Of these, 15 strains were suppressor mutations within *SAH1*. The remaining 101 strains were mutations in other genes, all of which were located at one locus and designated spontaneous suppressor growth delay in the *sah1* (*SSG1*). The *SSG1* mutant had a high intracellular SAM accumulation and prolonged CLS instead of RLS. Ogawa *et al*. (2016) found that this prolonged lifespan was attributed to the activation of SAM synthesis, reducing the amount of ATP (a substrate of SAM) and activated AMPK. Interestingly, WT cells, the supplementation of SAH in the medium increased intracellular SAM and activated AMPK, thereby extending the CLS (Ogawa *et al*., 2016). Furthermore, the WT cells accumulated SAH upon severe CR (0.05% Glucose), and accumulation of SAM and extension of maximum CLS were observed. It is likely that the effects of SAH also overlap with CR. However, the mechanism underlying the effect of SAH remains unclear.

Previously, Saito and Posas (2012) have found that strain deletion in *HOG1*, a stress-responsive MAP kinase, exhibits sensitivity to Ca^{2+} and osmotic pressure. To

investigate the relationship between Ca^{2+} signaling and lifespan, Kobayashi *et al*. (2008) screened for mutants that suppress the Ca^{2+} sensitivity exhibited by *hog1*Δ cells. As a result, the *sgh1–6* mutations were obtained from the *hog1*Δ cells. Among these mutations, *sgh3–6* suppressed not only the Ca^{2+} sensitivity but also the osmotic sensitivity in *hog1*Δ cells. Particularly, *sgh4* is a mutant allele of Whi3, a positive regulator of cell size control. Mizunuma *et al*. (2013) showed that whi3 is phosphorylated by the Ras/cAMP-dependent protein kinase A (PKA), involved in numerous cellular processes such as metabolism, stress resistance and proliferation, and PKA-dependent regulation. *sgh3, sgh5,* and *sgh6* are mutations in *TUP1*, *SKO1*, and *CYC8*, respectively. Sko1 forms a complex with Tup1–Cyc8 to inhibit gene transcription induced by hyperosmotic and oxidative stress; however, when responding to stress, the Sko1–Tup1–Cyc8 complex is phosphorylated by Hog1 to activate transcription (Rep *et al*., 2001; Proft and Struhl, 2002). Osmotic stress activates hyperosmotic signaling. Previously, it has been reported that activation of hyperosmotic signaling extends RLS through an increase in NAD^{+} and activation of *SIR2*, a component of CR, via glycerol synthesis (Kaeberlein *et al.,* 2002). However, the relationship between CLS and hyperosmotic signaling remains unclear.

Thus, both the hyperosmotic signaling pathway and SAH, which are predicted to be associated factors of the Ca^{2+} signaling pathway, were expected to extend lifespan related CR. Therefore, I focused on the molecular mechanisms that regulate lifespan as represented of CR in budding yeast to understand the molecular mechanisms involved in human aging and lifespan, and to prevent aging and diseases associated with aging. So, in Chapter 1, I investigated that inhibition of Sko1 function, a regulator of the high osmolarity glycerol (HOG) pathway, suppressed the oxidative stress susceptibility and shortened CLS of *hog1*Δ cells. In Chapter 2, I explored the mechanism of how SAH

administration to cells extends their CLS.

Chapter 1: *SKO1* deficiency extends chronological lifespan in *Saccharomyces cerevisiae*

1.1 Introduction

Cells of organisms are exposed to various stress stimuli such as osmotic pressure, oxidation, heat, heavy metals, and ultraviolet radiation. In response to such stress, to maintain proliferation, growth, and function, organisms have various mechanisms to sense these stresses and adapt to them. The HOG is a stress-responsive MAPK pathway that is activated to regulate hyperosmolarity. Its downstream factor Hog1 (MAP kinase) regulates various survival responses such as hyperosmolarity, oxidative stress, and cell cycle progression (Saito and Posas, 2012). Previously, Kobayashi *et al*. (2008) showed that the growth defect in *hog1*Δ cells with high osmolarity and high concentrations of $CaCl_2$ was restored by an additional mutation of the *tup1-484*, *sko1-18*, or *cyc8-389* gene. Sko1 is a repressor that mediates HOG pathway-dependent regulation in association with Tup1-Cyc8/Ssn6 and functions as a general repressor of the transcription of genes involved in a wide variety of processes, such as responding to osmotic and oxidative stress (Rep *et al*., 2001; Proft and Struhl, 2002). Alternatively, when cells perceive diverse stresses, the Sko1 complex is phosphorylated by Hog1, which activates transcription (Proft and Struhl, 2002). Previously, *sko1*Δ cells exhibited resistance to oxidative stress, and the sensitivity to oxidative stress exhibited by *hog1*Δ cells is suppressed by the loss of Sko1 function (Rep *et al*., 2001). In addition, *hog1*Δ cells exhibited shorter CLS, suggesting that the HOG pathway is a critical factor for cell survival. Herein, I analyzed the role of Sko1, a factor that suppresses the stress sensitivity of *hog1*Δ cells, in regulating lifespan.

1.2 Material and Methods

1.2.1. Yeast strains and media

Yeast strains used in this study are listed in Table 1. All yeast strains were derivatives of W303. Gene disruption was performed by a standard PCR-based method (Longtine *et al.*, 1998). Rich medium (YPD) consisted of 1% yeast extract (Oriental Yeast Co., Ltd.), 2% polypeptone (Shiotani M.S.), 2% glucose (Nacalai Tesque), 0.04% adenine hemisulfate (Sigma) and 0.02% uracil (Sigma).

1.2.2. Stress-resistance assay

Oxidative and osmotic stress-resistance assays were measured by spot assays. Cells suspended in water (5 x 10^7 cells/ml) were spotted onto YPD plates containing various concentrations of hydrogen peroxide (Santoku Chemical Industry) or KCl (Kanto Chemical). The cells were then grown at 25℃ for 3 or 4 days before visualization.

1.2.3 CLS assay

CLS analysis was performed in liquid Synthetic complete media SD, that adjusted to pH 6.0, as previously described (Fabrizio *et al*., 2003). SD contain 0.17% Yeast Nitrogen Base without Amino Acid (DIFCO), 0.5% ammonium sulfate (Sigma), amino acid (20 mg/1 contains adenine hemisulfate, 20 mg/1 uracil, 20 mg/1 tryptophan (Kanto Chemical), 20 mg/1 histidine (Sigma), 20 mg/1 arginine (Kanto Chemical), 20 mg/1 methionine (Nacalai Tesque), 30 mg/1 tyrosine (Sigma), 30 mg/1 leucine (Sigma), 30 mg/l isoleucine (Sigma), 30 mg/1 lysine (Sigma), 150 mg/1 valine (Sigma) and 60 mg/1 phenylalanine (Kanto Chemical), finally), 2% of glucose. Viability was measured by plating cells onto YPD plates and monitoring CFUs starting from day 3, which was

considered to be the initial survival (100%). All data were represented as the average of three independent experiments conducted at the same time.

1.2.4 Quantitative real-time PCR analysis

Cells were grown to log phase (2 x 10^6 cells/ml) in liquid SD medium at 25℃. Total RNA was isolated from cells using RNeasy Mini Kit (QIAGEN) and quantitative real-time PCR (qRT-PCR) was performed with One Step SYBR Prime Script RT-PCR Kit (Takara) using Light Cycler (Roche). PCR primers for *ACT1* as control were 5'-TTGGATTCCGGTG-ATGGTGTTACT-3' and 5'-TGAAGAAGATTGAGCAGCGGTTTG-3'. PCR primers for *GPD1* were 5'-GTATCTGTAGCCAATTGAAAGGTC-3' and 5'-CATTGAATACCT-AGTTCCTCAGTG-3'. PCR primers for *GPD2* were 5'-GACCATCCTATCAGAAGAT-CGGAC-3' and 5'-CTCTGGCTCGAAGATATGGGAATG -3' (Invitrogen).

1.2.5 Statistical analysis

All experiments were repeated at least twice with similar results each time. Data represent biological replicates. Appropriate statistical tests were used for every figure. GraphPad Prism 6 (GraphPad Software) was used for comparison of CLS, and *P* values were derived from a two-way ANOVA with time and strain used as independent factors. The qRT-PCR data were analyzed appropriate statistical tests (GraphPad Prism 9) as indicated in the figure legends.

1.3 Results

1.3.1 Effects of loss of function of repressors mediating HOG pathway-dependent regulation

Previously, we have obtained the *sko1-18*, *tup1-484*, and *cyc8-389* mutants, which suppress the Ca^{2+} sensitivity exhibited by *hog1*Δ cells, and we have created double mutants with *hog1*Δ cells to examine the growth phenotype of yeast cells. As previously reported (Rep *et al*., 2001), the *sko1-18* mutants suppressed the hydrogen peroxide sensitivity of *hog1*Δ cells, and the *tup1-484* or *cyc8-389* mutants partially suppressed it (Fig. 2A).

Extended lifespan is often correlated with increased tolerance to various stresses, including oxidative stress (Fontana *et al.*, 2010). So, I measured the CLS of *hog1*Δ cells, which are sensitive to osmotic pressure and oxidative stress, and found that *hog1*Δ cells exhibited a shortened lifespan, suggesting that the HOG pathway is essential for cell survival. Next, I measured CLS to determine whether the *sko1-18*, *tup1-484*, or *cyc8-389* mutants could also suppress the shortened CLS of *hog1*Δ cells. As a result, *sko1-18*, *tup1-484*, or *cyc8-389* mutants suppressed the shortened lifespan of *hog1*Δ cells and extended its lifespan to the same level as the wild-type strain (WT) (Fig. 2B). Loss of function due to deletion of Sko1 also suppressed the shortened lifespan of *hog1*Δ cells. Furthermore, the *hog1*Δ *sko1*Δ double mutant cells had a significantly longer lifespan than WT cells (Fig. 2C), suggesting that the Sko1 protein might play a role in lifespan.

1.3.2 Sko1 deficiency exhibits resistance to oxidative stress and lifespan extension via glycerol synthesis system

Since Sko1 was predicted to be involved in the regulation of lifespan, I next

examined whether a single *sko1*Δ cells would extend CLS. Strikingly, *sko1*Δ cells significantly extended CLS more than WT cells (Fig. 3A). The Sko1 protein forms a complex with Tup1-Cyc8 when the HOG pathway is inactive, inhibiting the transcription of hyperosmolarity and oxidative stress-inducible genes (Rep *et al*., 2001; Proft and Struhl, 2002). The extended lifespan exhibited by the *sko1*Δ cells suggests that the repression of target genes of Sko1 is derepressed. Previous reports have shown that hyperosmolarity extends RLS, which requires glycerol biosynthesis (Kaeberlein *et al.,* 2002). To determine whether CLS extension by *sko1*Δ cells was mediated by synthesized glycerol, I measured CLS by deleting *GPD1* and *GPD2*, which encode glycerol-3-phosphate dehydrogenase. CLS of *sko1*Δ *gpd1*Δ *gpd2*Δ triple mutants were equivalent to CLS of WT cells (Fig. 3A), suggesting that glycerol synthesis is essential for the lifespan extension in the *sko1*Δ cells.

Next, I tested the resistance to stress in *sko1*Δ *gpd1*Δ *gpd2*Δ triple mutants to examine whether the beneficial effect of deficient Sko1 function was due to enhanced glycerol synthesis (Fig. 3B). Resistance to osmotic (KCl) and hydrogen peroxide (H_2O_2) stress of *sko1*Δ cells was abolished by deletion of *GPD1* and *GPD2*, and the stress sensitivity of *sko1*Δ *gpd1*Δ *gpd2*Δ triple mutants were comparable to that of *gpd1*Δ *gpd2*Δ double mutants (Fig. 3B). Overall, glycerol synthesis may be an important downstream factor mediating the effects of *sko1*Δ cells on CLS extension and stress tolerance. Therefore, I measured the transcript levels of *GPD1* and *GPD2* by quantitative real-time PCR in *sko1*Δ cells to see if the loss of Sko1 function derepressed the glycerol synthesis gene (Fig. 3C, D). The amount of *GPD1* transcript level in the *sko1*Δ cells was increased approximately 1.8-fold change compared to WT cells, suggesting that loss of Sko1 function released the repression of *GPD1* expression. On the other hand, there was no

change in the amount of *GPD2* transcription, indicating that Sko1 was expected to more strongly inhibit *GPD1* transcription.

1.3.3 Lifespan extension of Sko1 deficiency is an alternative pathway to osmotic stress

During hyperosmotic stress, cells activate the HOG pathway and phosphorylate the Sko1-Tup1-Cyc8 complex, thereby suppressing Sko1 function (Proft and Struhl, 2002). Since hyperosmolarity is known to extend CLS (Smith *et al*., 2007), I analyzed whether the extension of CLS in *sko1*Δ cells is associated with hyperosmolarity. Consistent with a previous report (Smith *et al*., 2007), I found that treatment with hyperosmolarity (sorbitol) appears to extend CLS in WT cells (Fig. 4). I also noted that hyperosmolarity significantly increased the CLS of *sko1*Δ cells early and mid-life (up to 20 days) compared to the CLS of WT cells under osmotic stress conditions (Fig. 4). These data indicated that CLS extension by *sko1*Δ cells or osmotic stress acts via a branching pathway.

1.4 Discussion

In this chapter, I analyzed the role of Sko1 in suppressing the stress sensitivity of *hog1*Δ cells, and the high survival rate of the *sko1*Δ cells was dependent on glycerol synthesis. Moreover, the resistance to stress and high survival rate exhibited by the *sko1*Δ cells were suppressed in *sko1*Δ *gpd1*Δ *gpd2*Δ triple mutants (Fig. 3A, B). Therefore, glycerol synthesis is critical for the high survival rate of *sko1*Δ cells. However, because of the negative feedback in the HOG pathway (Yamamoto *et al*., 2010), it is expected that constant transcriptional activation by Sko1 deletion would also have a negative effect on the lifespan. Thus, the regulation of lifespan requires not only simple gene activity but also elaborate regulation of gene activity. In addition, quantitative PCR results showed that *GPD1* transcription was increased in the *sko1*Δ cells (Fig. 3C). These results suggest that the *GPD* gene is critical for lifespan extension and resistance to stress due to the loss of Sko1 function. The target genes of Sko1 are *GRE2*, *AHP1*, *SFA1*, *GLR1*, and *YML131W*, which protect against oxidative stress and are repressed by Sko1 in non-stressed conditions (Rep *et al*., 2001). However, further analysis is needed to determine if the lifespan extension of the *sko1*Δ cells depend on these factors.

Curiously, although the *sko1*Δ cells suppressed the growth defect of *hog1*Δ cells under hyperosmotic stress conditions (Rep *et al*., 2001), *sko1*Δ cells did not exhibit clear resistance to osmotic stress conditions (Fig. 3B). Thus, there is little beneficial effect of *sko1*Δ cells on the WT background of nutrient growth under osmotic stress conditions. This is consistent with the results of partial extension of lifespan when hyperosmotic pressure was applied to the *sko1*Δ cells (Fig. 4), suggesting that the response to hyperosmolarity and the regulation of gene expression by deletion of *SKO1* are divergent pathways in part.

Herein, the *tup1-484/scz3* and *cyc8-389/scz6* mutations were also factors suppressing Ca^{2+} sensitivity in *hog1*Δ cells; however, because both *hog1*Δ *tup1*Δ and *hog1*Δ *cyc8*Δ double mutants are highly aggregative (data not shown), they were not available for further analysis.

Identification of the actual effector mechanisms by which loss of *SKO1* protects against chronological aging is a critical future challenge. During ethanol fermentation, yeast cells encounter osmotic, oxidative, and ethanol stresses. Thus, the findings in this study might be useful to produce strains that are tolerant to these fermentation-associated stresses.

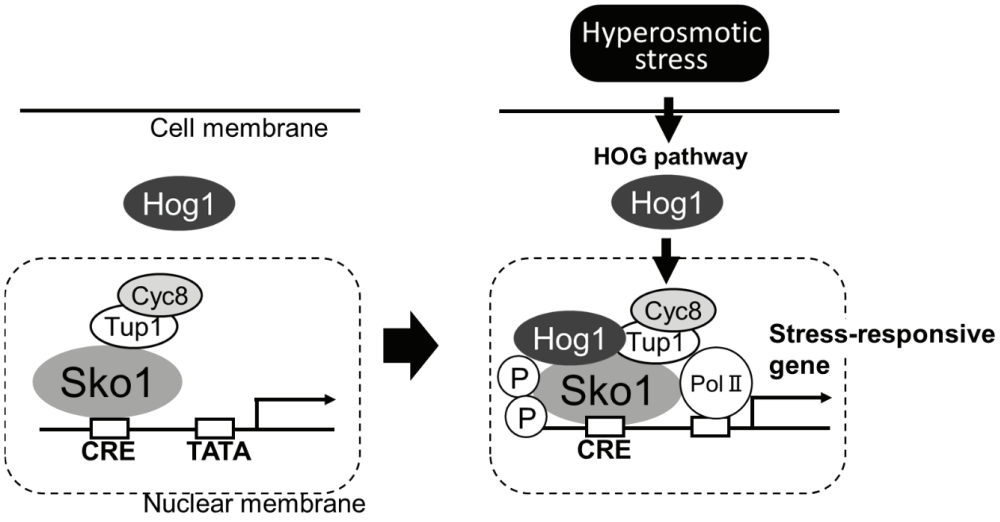

Fig. 1 Regulation of the Sko1-Tup1-Cyc8 complex by Hog1.

(1) Under normal conditions without stress, the Sko1-Tup1-Cyc8 complex binds to CRE (cyclic-AMP responsive element), upstream of stress-inducible genes, and represses transcription. (2) When cells sense hyperosmotic stress, Hog1 migrates to the nucleus and phosphorylates Sko1. Then, the phosphorylated Sko1-Cyc8-Tup1 complex is repressed and mobilizes RNA polymerase II (Pol II) to activate transcription

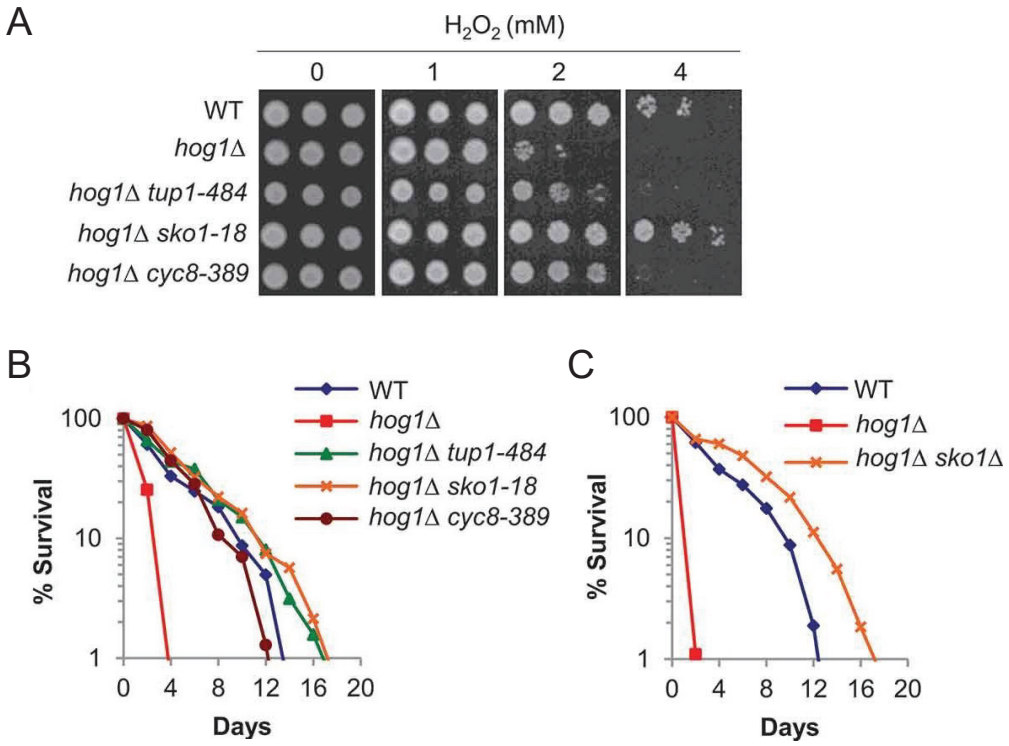

Fig. 2 Deletion of *SKO1* suppressed *hog1*Δ sensitivity to oxidative stress and extended lifespan.

(A) Growth of various strains on solid YPD medium containing the indicated concentrations of hydrogen peroxide. Ten-fold serially diluted cells of WT, *hog1*Δ, *hog1* Δ *tup1-484, hog1*Δ *sko1-18, and hog1*Δ *cyc8-389* were spotted onto YPD solid medium containing various concentrations of hydrogen peroxide. The cells were then grown at 25ºC for 3 days before visualization. (B) CLS curves for WT, *hog1*Δ, *hog1*Δ *tup1-484, hog1*Δ *sko1-18*, and *hog1*Δ *cyc8-389* are shown. (C) CLS curves of WT, *hog1*Δ, and *hog1*Δ *sko1* are shown.

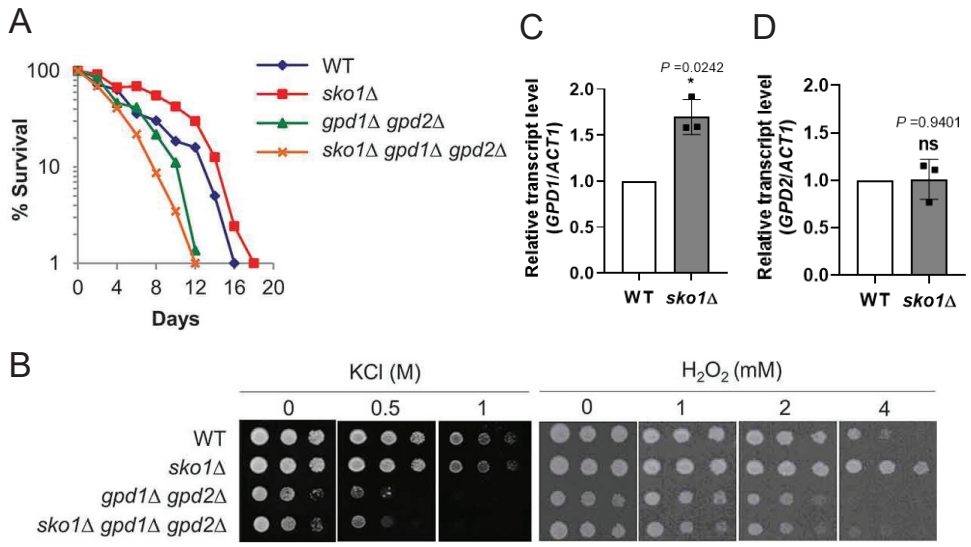

Fig. 3 Glycerol Synthesis System is required for resistance to oxidative stress and lifespan extension in *sko1*Δ.

(A) CLS curves for WT, *sko1*Δ, *gpd1*Δ *gpd2*Δ, and *sko1*Δ *gpd1*Δ *gpd2*Δ are shown. (B) Osmotic (KCl) (left panel) and hydrogen peroxide (right panel) test. Ten-fold serially diluted cells of WT, *sko1*Δ, *gpd1*Δ *gpd2*Δ, and *sko1*Δ *gpd1*Δ *gpd2*Δ were spotted onto solid medium containing KCl or hydrogen peroxide at 25ºC and incubated for 3 days. (C, D) Relative expression level of (C) *GPD1* and (D) *GPD2* in WT, *sko1*Δ measured by reverse transcription Real-Time PCR. Mean ± SD (n = 3), two-sided unpaired t-test; ns, not significant.

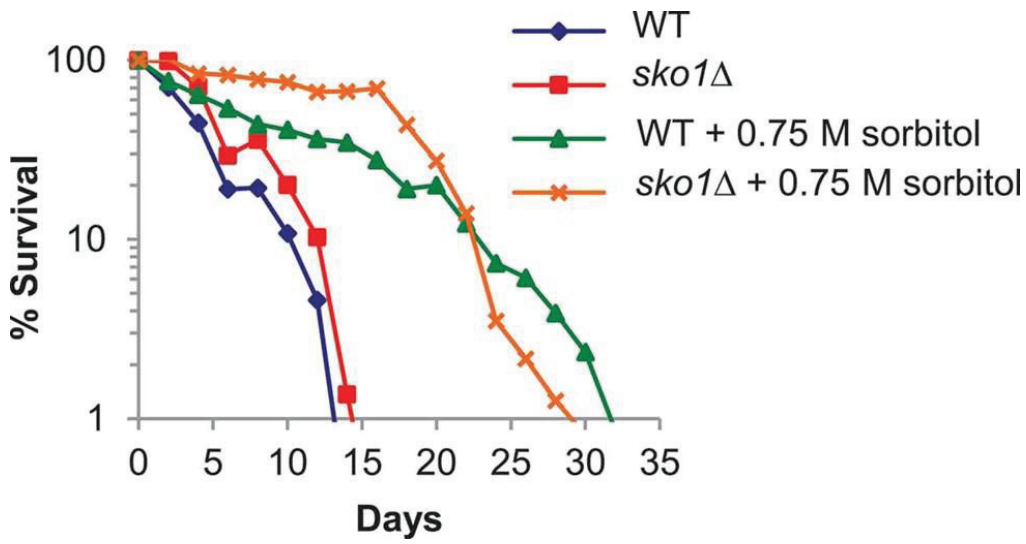

Fig. 4 Lifespan extension of *sko1*Δ is a partially separate pathway from that induced by hyperosmolarity.

CLS curves for WT and *sko1*Δ in the presence or absence of hyperosmolarity (0.75 M sorbitol) are shown.

Table 1 Strains used in Chapter 1

Strain	**Name**	**Genotype**	**Source of Reference**
W303-1A	WT	*MATa* ; *trp1-1 leu2-3,112 ade2-1 ura3-1 his3-11,15 can1-100*	NBRP/YGRP
YFK100	*hog1* Δ	*MATa* ; *hog1* Δ*::TRP1*	Lab. Stock
YFK71	*hog1* Δ *sko1-18*	*MATa* ; *hog1* Δ*::TRP1 sko1-18*	Lab. Stock
YFK66	*hog1* Δ *tup1-484*	*MATa* ; *hog1* Δ*::TRP1 tup1-484*	Lab. Stock
YFK75	*hog1* Δ *cyc8-389*	*MATa* ; *hog1* Δ*::TRP1 cyc8-389*	Lab. Stock
YFK73	*hog1* Δ *sko1* Δ	*MATa* ; *hog1* Δ*::TRP1 sko1* Δ*::kanMX4*	Lab. Stock
YAL12	*sko1* Δ	*MATa* ; *sko1* Δ*::kanMX4*	Lab. Stock
YAL18	*gpd1* Δ *gpd2* Δ	*MATa* ; *gpd1* Δ*::kanMX4 gpd2* Δ*::kanMX4*	Lab. Stock
YAL26	*sko1* Δ *gpd1* Δ *gpd2* Δ	*MATa* ; *sko1* Δ*::kanMX4 gpd1* Δ*::kanMX4 gpd2* Δ*::kanMX4*	Lab. Stock

Table 2 *P* value for CLS analysis in Chapter 1

Figure	**Strain A**	**Strain B**	***P*-value against B**
2B	WT	*hog1* Δ	**<0.001**
	hog1 Δ	*hog1* Δ *sko1-18*	**<0.001**
	hog1 Δ	*hog1* Δ *tup1-484*	**<0.001**
	hog1 Δ	*hog1* Δ *cyc8-389*	**<0.001**
2C	WT	*hog1* Δ *sko1* Δ	**<0.001**
	hog1 Δ	*hog1* Δ *sko1* Δ	**<0.001**
3A	WT	*sko1* Δ	**<0.001**
	WT	*gpd1* Δ *gpd2* Δ	0.0686
	sko1 Δ	*sko1* Δ *gpd1* Δ *gpd2* Δ	**<0.001**
4	WT	WT (Glycerol 0.75 M)	**<0.001**
	sko1 Δ	*sko1* Δ (Glycerol 0.75 M)	**<0.001**

P value were derived from a two-way ANOVA with time and strain used as independent factors.

Chapter 2: *S*-adenosyl-L-homocysteine extends lifespan through methionine restriction effects methionine restriction

2.1 Introduction

As people live longer, research has turned to finding ways to extend life while avoiding the diseases and infirmities of advanced age, particularly through the study of diet at a basic level. Dietary restriction such as MetR is an effective strategy to promote longevity and counteract age-related morbidities (Ables and Johnson, 2017; Parkhitko *et al*., 2019). So far, genetic manipulation or pharmacological inhibition of Met metabolic pathways (Annibal *et al*., 2021; Hepowit *et al*., 2021; Johnson and Johnson, 2014; Obata and Miura, 2015; Ogawa *et al*., 2016; Ruckenstuhl *et al*., 2014) and a Met-restricted diet extend lifespan (Orentreich *et al*., 1993; Wu *et al*., 2013); however, it is not practical to apply these interventions in humans. Previously, Ogawa *et al*. (2016) have found that supplementation with SAH, an endogenous Met derivative, activates the energy sensor AMPK and extends lifespan in yeast (Fig. 5). SAH treatment triggered high accumulation of SAM, which may be attributed to the consumption of ATP and the induction of AMPK activation. However, the details of the mechanism of lifespan extension using SAH are unknown. Here, I discovered that the intake of SAH reduces intracellular Met and induces benefits that mimic MetR in budding yeast *Saccharomyces cerevisiae*. In addition, treatment with SAH activates AMPK and mimics some of the benefits of MetR.

2.2 Material and Methods

2. 2. 1. Yeast strains and media

Yeast strains used in this study are listed in Table 3. All yeast strains were derivatives of W303. Gene disruption was performed by a standard PCR-based method (Longtine *et al*., 1998). SD contain 0.17% Yeast Nitrogen Base without Amino Acid (DIFCO), 0.5% ammonium sulfate (Sigma), amino acid (20 mg/1 contains adenine hemisulfate, 20 mg/1 uracil, 20 mg/1 tryptophan (Kanto Chemical), 20 mg/1 histidine (Sigma), 20 mg/1 arginine (Kanto Chemical), 20 mg/1 methionine (Nacalai Tesque), 30 mg/1 tyrosine (Sigma), 30 mg/1 leucine (Sigma), 30 mg/l isoleucine (Sigma), 30 mg/1 lysine (Sigma), 150 mg/1 valine (Sigma) and 60 mg/1 phenylalanine (Kanto Chemical), finally), 2% of glucose.

2.2.2. CLS assay

Described in 1. 2. 3.

2.2.3. Growth conditions for metabolome analysis of yeast

WT cells were cultured in SDC liquid medium. Cells were grown to log phase (OD600 nm = 0.2) in SDC liquid medium at 25℃. SAH was added to SDC medium to 1 mM and cultured for another eight hours (OD600 nm = 0.4). As a control, cells were grown log phase in SDC medium at 25℃ (OD600 nm = 0.4).

2.2.4. Extraction of the intracellular metabolite from yeast

Metabolite extraction was conducted using the previously described modification (Soga *et al*., 2003). Cells were harvested from the culture medium (OD600 nm = 30) and filtered

through a 0.45 μm pore size filter. The internal cationic and anionic standards were methionine sulfone and 2-morpholinoethanesulfonic acid, respectively. The lyophilized samples were dissolved in 50 μl Milli-Q water and subjected to capillary electrophoresis-time-of-flight mass spectrometry (CE-TOFMS) analysis.

2.2.5. Method for metabolome analysis

Instrumentation: All capillary electrophoresis mass spectrometry (CE-MS) experiments were conducted using Agilent 7100 CE capillary electrophoresis (Agilent Technologies, Waldbronn, Germany), Agilent 6230 LC/MSD TOF system (Agilent Technologies, Palo Alto, CA, USA), an Agilent1100 series binary HPLC pump, and the G1603A Agilent CE-MS adapter- and G1607A Agilent CE-ESI-MS sprayer kit. For anionic metabolite analysis, the original Agilent stainless Electrospray ionization (ESI) needle was replaced with the Agilent G7100-60041 platinum ESI needle (Soga *et al*., 2009). Agilent MassHunter Workstation was used to conduct system control and data acquisition, and data analysis was done using the Keio MasterHands software.

Cationic metabolite analysis by CE-MS: Separations were conducted in a fused silica capillary (50 mm i.d. x 100 cm total length) filled with 1 M formic acid as the electrolyte (Soga *et al*., 2003; Soga *et al*., 2006). About 5 nl sample solution was injected at 50 mbar for five seconds, and 30 kV of voltage was applied. The capillary temperature was maintained at 20°C and the sample tray was cooled below 5°C. Methanol-water (50% v/v) containing 0.01 mM Hexakis (2,2-difluoroethoxy) phosphazene was delivered as the sheath liquid at 10 μl/min. ESI-time-of-flight mass spectrometry (ESI-TOFMS) was performed in the positive ion mode and the capillary voltage was set at 4,000 V. A flow

rate of heated dry nitrogen gas (heater temperature 300°C) was maintained at 7 psig. In TOFMS, the fragmentor-, skimmer-, and Oct RFV voltage were set at 75 V, 50 V, and 500 V, respectively. Automatic recalibration of each acquired spectrum was conducted using reference masses of reference standards. The ^{13}C isotopic ion of a protonated methanol dimer ($[2MeOH + H]^+$, m/z 66.0631) and Hexakis(2,2-difluoroethoxy)phosphazene ($[M + H]^+$, m/z 622.0290) provided the lock mass for exact mass measurements (Satoh *et al*., 2017).

Anionic metabolite analysis by CE-MS: A commercially available COSMO(+) (chemically coated with cationic polymer) capillary (50 mm i.d. x 105 cm total length) (Nacalai Tesque) was used with a 50 mM ammonium acetate solution (pH 8.5) as the electrolyte (Satoh *et al*., 2017; Soga *et al*., 2009). Sample solution (30 nl) was injected at 50 mbar for 30 sec and -30 kV of voltage was applied. Ammonium acetate (5 mM) in 50% methanol-water (v/v) containing 0.01 mM Hexakis(2,2-difluoroethoxy)phosphazene was delivered as the sheath liquid at 10 µl/min. ESI-TOFMS was conducted in the negative ion mode; the capillary voltage was set at 3,500 V. For TOFMS, the fragmentor-, skimmer-, and Oct RFV voltage were set at 100 V, 50 V, and 500 V, respectively. Automatic recalibration of each acquired spectrum was conducted using reference masses of reference standards, i.e., ^{13}C isotopic ion of deprotonated acetic acid dimer ($[2CH_3COOH-H]^-$, m/z 120.0384), and Hexakis + deprotonated acetic acid (m/z 680.03554) provided the lock mass for exact mass measurements.

Statistical analysis: MetaboAnalyst software ver. 5.0 was used for statistical analysis (Pang *et al*., 2021). Categories that have missing values were excluded. Data scaling was

performed with mean-centered and divided by the standard deviation of each variable.

2.2.6. Growth conditions with [methyl-^{13}C]Met for metabolome analysis of yeast

WT cells were preincubated in SD-Met liquid medium containing 20 mg/L [methyl-^{13}C]Met (Cambridge Isotope Laboratories) at 25℃ overnight. The cells were then grown in a fresh SD-Met liquid medium containing 20 mg/L [methyl-^{13}C]Met liquid medium at 25℃ until the logarithmic growth phase (OD600 nm = 0.2). These procedures were designed to ensure that the only external source of Met was [methyl-^{13}C]Met. The culture medium was then split into two, and 1 mM SAH solution was added to one of them, and the cells were cultured for another eight hours (OD600 nm = 0.4). The other was used as a control and cultured until the logarithmic growth phase (OD600 nm = 0.4). The [methyl-^{13}C]Met and [methyl-^{13}C]SAM content were expressed as nmol per mg dry cell weight (DCW).

2.2.7 Extraction of intracellular [methyl-^{13}C]Met and [methyl-^{13}C]SAM from yeast

Extraction of SAM and SAH was conducted as previously described (Christopher *et al*., 2002). The cells were harvested (total OD600 nm = 15), washed twice with 20 ml cold water, and then extracted with 1 ml 10% perchloric acid (Fujifilm Wako Chemical) for one hour at room temperature. The supernatant was diluted with MilliQ-grade water, and the samples were filtered for CE-TOFMS.

2.2.8 GFP-ATG8 processing assay

Cells harboring the GFP-Atg8 expressing plasmid were grown to log phase (OD600 nm = 0.2) in liquid SD medium lacking uracil at 25ºC. SAH solution was added to SDC

medium to 1 mM, and the cells were incubated for another eight hours (OD600 nm = 0.4). For the control, cells were grown to log phase (OD600 nm = 0.4) in liquid SDC medium at 25ºC. Cells growth was stopped by adding TCA (Sigma) to about 9% final concentration and putting on ice for at least five minutes before cells were pelleted. The cells were obtained by centrifugation, washed twice with cold acetone (Nacalai Tesque), and dried in a speed-vac. Pellets were resuspended in 100 µl of urea buffer (50 mM Tris (Sigma) [pH 7.5], 1 mM EDTA (Sigma), 6 M urea (Kanto Chemical), 1% SDS (Nacalai Tesque), 1 mM PMSF (Sigma), 1x complete protease inhibitor cocktail (Roche), and 0.1% Tween 20 (Bio-Rad)) and lysed by vortexing with an equal volume of glass beads at room temperature, with subsequent heating for ten minutes at 65ºC. Further analysis was conducted using SDS-PAGE and immunoblotting using anti-GFP antibody (Roche, 1:1000) and anti-PSTAIR antibody (Novus bio., 1:1000). ImageJ was used to quantify signals for Western blotting results, and GraphPad Prism 9 was used for statistical analysis.

2.2.9 Detection of Rps6 activation

WT cells were grown to log phase (OD600 nm = 0.2) in the SDC liquid medium at 25°C. SAH was added to SDC medium to 1 mM and cultured for another eight hours (OD600 nm = 0.4). As a control, cells were grown log phase in SDC medium at 25°C (OD600 nm = 0.4). Cells were then harvested, washed with 1ml TEG +PPi buffer (50 mM Tris (Sigma)-HCl (Nacalai Tesque), 1 mM EDTA (Sigma) [pH 7.5], 10% glycerol (Nacalai Tesque), 30 mM NaCl (Nacalai Tesque), 10 mM NaF (Fujifilm Wako Chemical), 1 mM sodium orthovanadate (Na_3VO_4) (Fujifilm Wako Chemical), 1 mM PMSF (Sigma), 1 mM DTT (Nacalai Tesque), 1x complete protease inhibitor cocktail (Roche), and 0.1% Tween 20 (Bio-Rad)). The precipitate was frozen in liquid nitrogen and stored at -80°C. The

frozen precipitate was dissolved on ice and gently resuspended in SDS-PAGE sample buffer, and boiled for ten minutes. The eluted proteins were resolved by SDS-PAGE and detected by anti-Phospho-S6 Ribosomal Protein (Ser235/236) antibody (Cell signaling Tech., 1:1000) and anti- PSTAIR antibody (Novus bio., 1:1000). ImageJ (NIH) was used to quantify signals for Western blotting results, and GraphPad Prism 9 (GraphPad Software) was used for statistical analysis.

2.3 Results

2.3.1 Intracellular methionine levels are prominently reduced when cells are supplemented with SAH

To investigate the basis for the extension of yeast cell lifespan when supplemented with SAH, I performed a metabolomics analysis of WT with or without SAH treatment. However, because SAH treated cells have a slower growth rate than untreated cells (Fig. 6), the comparison was made with cells cultured to the same OD600 value (about 0.4) rather than cells cultured at the same time. Here, a total of 148 metabolites were identified (Table 4). Of these, 63 metabolites were significantly up-regulated and 6 were down-regulated (Fig. 7A-C, Table 4). As previously reported, administration of SAH increased not only SAH but also SAM (Ogawa *et al*., 2016). Because SAH is a potent competitive inhibitor of SAM, the major methyl group donor in organism, intracellular SAH must be rapidly degraded by the SAH hydrolase *SAH1* (Christopher *et al*., 2002). Therefore, accumulation of SAH has a negative effect on cell proliferation. Previously, Mizunuma *et al.* (2004) have found that exogenous SAM significantly improved the growth of *sah1*, a mutant allele of the *SAH1* gene that accumulates high levels of SAH. Therefore, I speculate that the increase in SAM levels by SAH supplementation may be the result of up-regulation of SAM synthesis from Met by an unknown mechanism that acts to counteract the effects of SAH. Since SAM is biosynthesized from Met and ATP, activation of SAM synthesis would be expected to decrease intracellular Met levels. As expected, only methionine was significantly reduced among the amino acids in SAH treated cells (Fig. 7D).

2.3.2 SAH promotes SAM synthesis and decreases amount of Met

Next, to investigate whether the decrease in intracellular Met was due to accelerated consumption, I switched the L-Met in the culture medium to L-[methyl-^{13}C]Met and the fate of [methyl-^{13}C]Met with or without SAH treatment were chased. As a result, supplementation with SAH significantly decreased intracellular [methyl-^{13}C]Met and increased [methyl-^{13}C]SAM compared to the vehicle-treated control cells (Fig. 8A, B). Furthermore, extracellular metabolomic data showed that [methyl-^{13}C]Met levels after supplementation with SAH were slightly lower than in the medium of control cells, but were still sufficiently present (Fig. 8C). These results suggest that SAH promotes Met reduction by converting endogenous Met to SAM, although I cannot exclude the possibility that SAH inhibits SAM degradation.

The lower Met content in SAH treated cells suggests that longevity that derives from SAH supplementation may involve a MetR-like state. Because high concentrations of Met have been reported to shorten lifespan (Wu *et al*., 2013), if the lifespan extension effect of SAH is due to Met reduction, it would be expected that excess Met would block lifespan extension by SAH. Therefore, I evaluated the effect of the excess amount of Met on the CLS. As expected, high concentrations of Met (10x Met) partially suppressed lifespan extension when supplemented with SAH (Fig. 8D). Collectively, these results indicate that SAH extends lifespan by reducing Met.

2.3.3 SAH treatment inactivate mTORC1 and promote autophagy

Given that Met inhibits autophagy and MetR extends CLS (Fabrizio and Longo, 2007) in an autophagy-dependent manner (Plummer and Johnson, 2019; Ruckenstuhl *et al*., 2014), I hypothesized that SAH might promote autophagy. The GFP-ATG8 cleavage assay (Nair *et al*., 2011), which assesses the autophagy-dependent cleavage of GFP-Atg8

within the vacuole, can be used to monitor bulk autophagy progression in SAH treated cells. The WT strains showed little autophagy activity during the logarithmic phase on SDC medium (Fig. 9A). On the other hand, bulk autophagy was induced by exposure of cells to SAH media during the logarithmic phase.

Since mTORC1 inhibits autophagy (Shimobayashi and Hall, 2014), I expected SAH to inhibit mTORC1 function. Thus, I investigated the effect of SAH treatment on the phosphorylation level of Rps6 (a homolog of mammalian S6), a downstream target kinase of mTORC1 (Wullschleger and Hall, 2006). In the logarithmic growth phase of WT strains, supplementation with SAH reduced the phosphorylation of Rps6, which correlated with its kinase activity (Fig. 9B), suggesting that SAH reduces levels of mTORC1 activity. Moreover, I examined if SAH extends CLS by mechanisms requiring mTORC1 and autophagy. The extended CLS of *tor1*Δ cells were further enhanced when SAH was added, but it was like that of WT treated with SAH, suggesting that SAH may be involved in lifespan extension, at least in part, through inhibition of mTORC1 (Fig. 9C). Furthermore, when the *ATG7* gene, which encodes an essential component of the autophagic machinery, was deleted, SAH decreased the death rate of *atg7*Δ cells during the early period of the lifespan (around 2 days), but overall, the CLS of *atg7*Δ cells reduced (Fig. 9C). This suggests that autophagy is required for the sustained lifespan extension by SAH.

2.4 Discussion

In this chapter, I discussed that supplementation with SAH reduces intracellular Met levels by promoting SAM synthesis. Supplementation with SAH mimicked the physiological phenomenon that occurs during MetR, inhibiting the activity of mTORC1, the major nutrient-sensing pathway of the organism, and promoting autophagy activity. The effects of SAH can possibly explain how the high accumulation of SAM leads to the consumption of Met and ATP, which in turn induces the inactivation of mTORC1 and the activation of AMPK, respectively. Although there seem to be a contradiction between SAM synthesis consuming Met and ATP and the increase in ATP levels (Fig. 7A, C), previous results by Ogawa *et al*. (2016) suggested that this was probably the result of the action of an unknown mechanism by which AMPK compensates for the consumption of ATP. To compensate for consumed ATP, the activation of AMPK by supplementation with SAH is also suggested to affect mitochondrial function, the major source of ATP in an organism. In fact, metabolomic analysis suggests that SAH-treated cells have increased metabolites in the TCA cycle, such as citric acid, fumaric acid, and malic acid, thereby increasing mitochondrial activity (Fig. 7A, C).

Considering that glucose restriction (0.5% glucose) is associated with MetR (Zou *et al*., 2020) and physiological increases in SAH levels have been reported in even lower (0.05%) glucose-treated yeast cells (Ogawa *et al*., 2016), it is likely that the effects of SAH also overlap with CR. Therefore, metabolomic analysis showed that supplementation with SAH increased NAD^+, which activates the sirtuin gene, a component of CR (Bonkowski and Sinclair, 2016) (Fig. 7A, Table 4). In addition, spermidine, a natural polyamine that mimics CR, was increased (Eisenberg *et al*., 2009) (Fig. 7A, C, Table 4). These results suggest that SAH mimics some effects of CR as well

as MetR (Fig. 10).

While SAH inhibits the methylation reaction of SAM, this study shows that SAH is also promotes SAM synthesis. However, it unknown how SAH activates SAM synthesis. Christopher *et al*. (2002) proposed that the SAM/SAH ratio is important for cell growth, and a decrease in this ratio inhibits growth. Therefore, the supplementation of SAH may be a kind of hormesis to counteract the decrease in the SAM/SAH ratio and promote SAM synthesis. To apply the benefits of SAH treatment in lifespan extension more safely and effectively to humans, it is a future issue to investigate in detail the metabolic changes and molecular mechanisms of cells treated with SAH.

Although consuming a Met-restricted diet or the reduction of Met or ATP by inhibiting their respective synthetic enzymes can have benefits such as extending lifespan, the finding that SAH, a metabolite of organism, affects Met and ATP levels provides new insights in terms of their consumption. Moreover, Ogawa *et al*. (2022) found that SAH treatment extends lifespan in *Caenorhabditis elegans*, a multicellular model organism, by activating AMPK and the benefits of MetR. Accordingly, MetR extends the lifespan of many species, and exposure to SAH is expected to have various benefits across evolutionary boundaries.

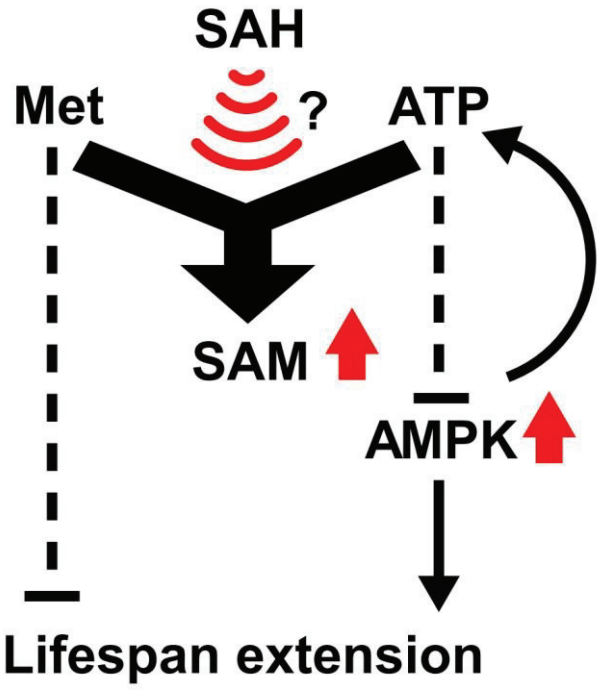

Fig. 5 Stimulating SAM synthesis activates AMPK and extends lifespan.

Model for yeast longevity mediated by the stimulation of SAM synthesis by SAH.

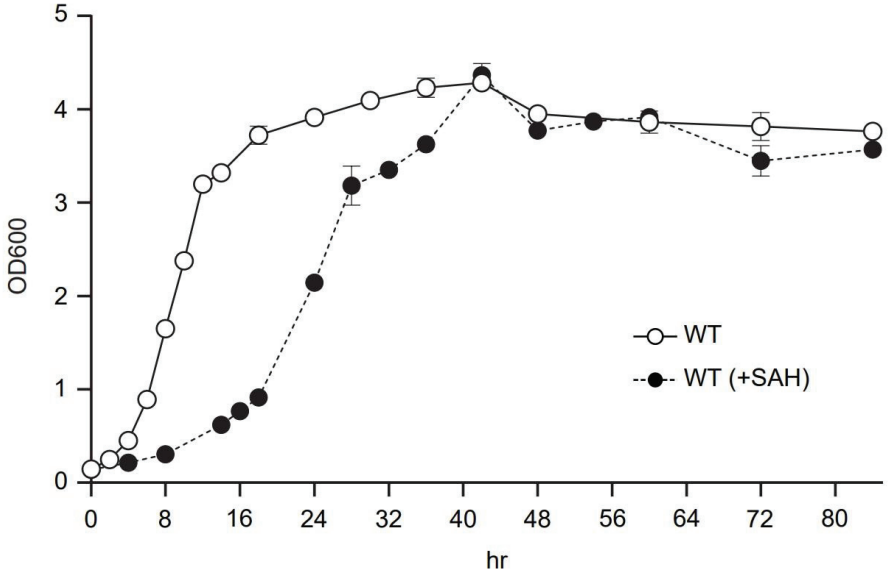

Fig. 6 Growth rate of SAH treated cells

Growth rate and cell density of WT cells with (closed circle) or without (opened circle) SAH treatment is shown. WT cells cultured in an SDC medium to log phase (OD600 nm = 0.2) were further cultured with or without 1 mM SAH. A representative set of data from two biological repeats is shown. Mean ± S.D. (n = 3).

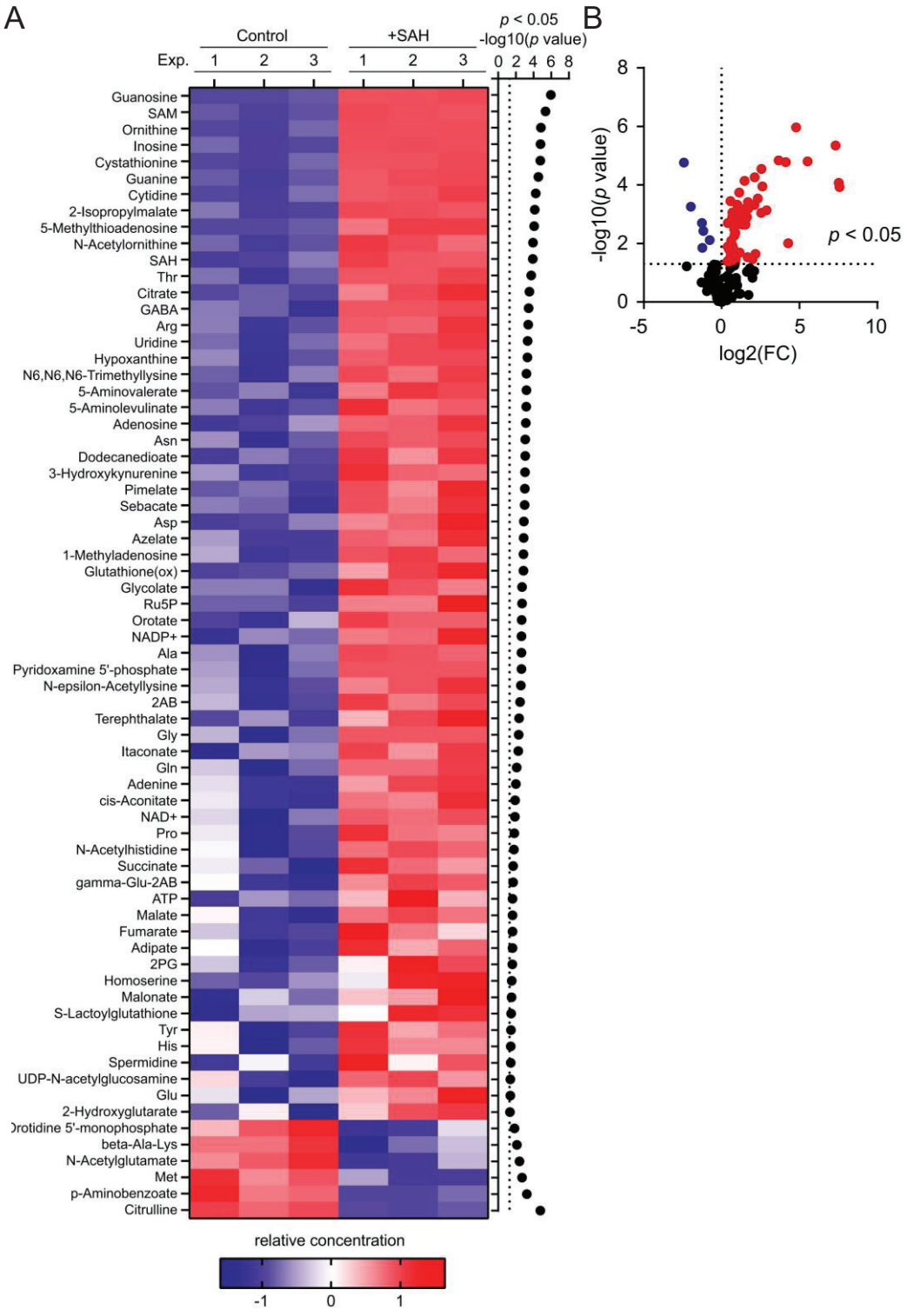
A
Control
+SAH
Exp.
1 2 3 1 2 3
p < 0.05
-log10(p value)
0 2 4 6 8
Guanosine
SAM
Ornithine
Inosine
Cystathionine
Guanine
Cytidine
2-Isopropylmalate
5-Methylthioadenosine
N-Acetylornithine
SAH
Thr
Citrate
GABA
Arg
Uridine
Hypoxanthine
N6,N6,N6-Trimethyllysine
5-Aminovalerate
5-Aminolevulinate
Adenosine
Asn
Dodecanedioate
3-Hydroxykynurenine
Pimelate
Sebacate
Asp
Azelate
1-Methyladenosine
Glutathione(ox)
Glycolate
Ru5P
Orotate
NADP+
Ala
Pyridoxamine 5'-phosphate
N-epsilon-Acetyllysine
2AB
Terephthalate
Gly
Itaconate
Gln
Adenine
cis-Aconitate
NAD+
Pro
N-Acetylhistidine
Succinate
gamma-Glu-2AB
ATP
Malate
Fumarate
Adipate
2PG
Homoserine
Malonate
S-Lactoylglutathione
Tyr
His
Spermidine
UDP-N-acetylglucosamine
Glu
2-Hydroxyglutarate
Orotidine 5'-monophosphate
beta-Ala-Lys
N-Acetylglutamate
Met
p-Aminobenzoate
Citrulline
relative concentration
-1 0 1
B
-log10(p value)
8 6 4 2 0
p < 0.05
-5 0 5 10
log2(FC)

C

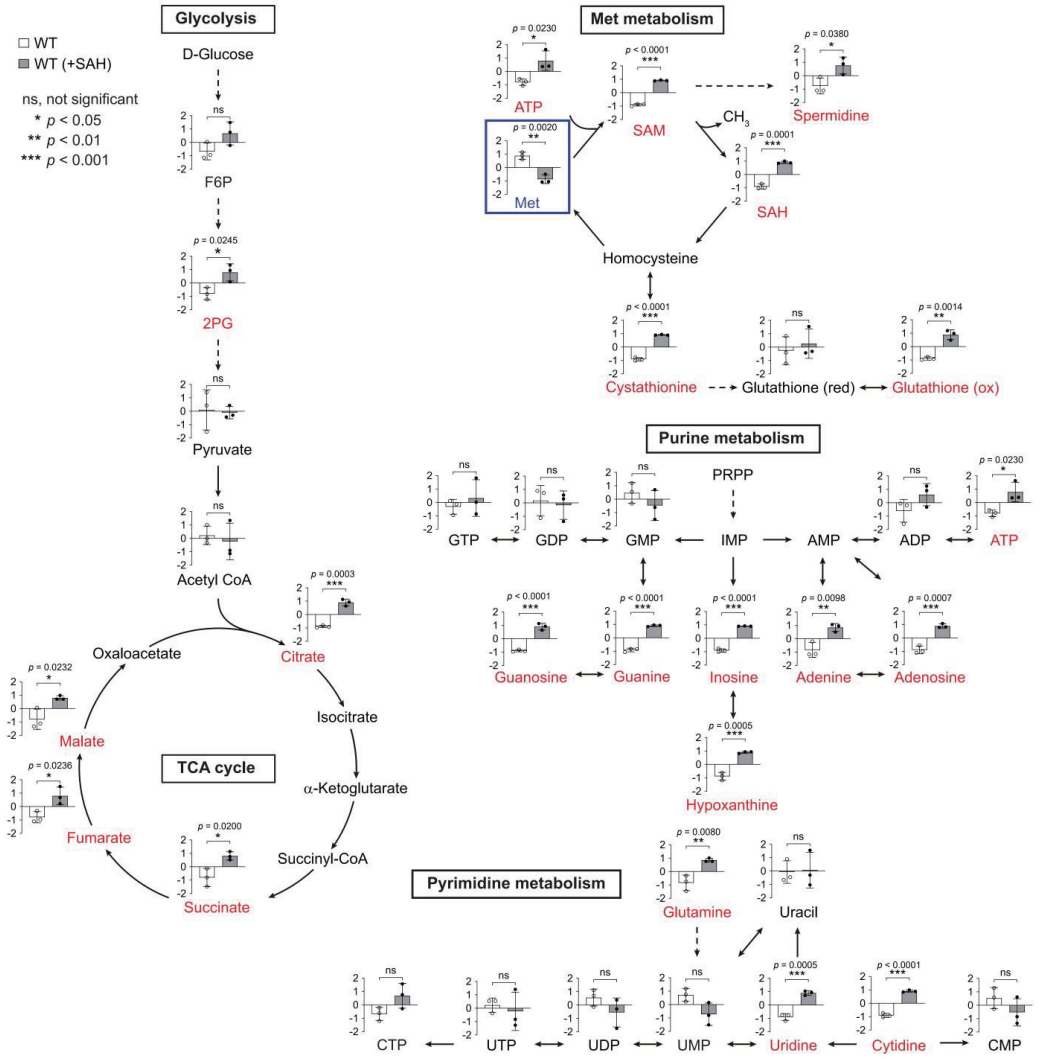
WT
WT (+SAH)
ns, not significant
* p < 0.05
** p < 0.01
*** p < 0.001
Glycolysis
D-Glucose
F6P
2PG
Pyruvate
Acetyl CoA
Citrate
Isocitrate
α-Ketoglutarate
Succinyl-CoA
Succinate
Fumarate
Malate
Oxaloacetate
TCA cycle
Met metabolism
ATP
Met
SAM
SAH
Spermidine
Homocysteine
Cystathionine
Glutathione (red)
Glutathione (ox)
Purine metabolism
PRPP
GTP
GDP
GMP
IMP
AMP
ADP
ATP
Guanosine
Guanine
Inosine
Adenine
Adenosine
Hypoxanthine
Pyrimidine metabolism
Glutamine
Uracil
CTP
UTP
UDP
UMP
Uridine
Cytidine
CMP

D

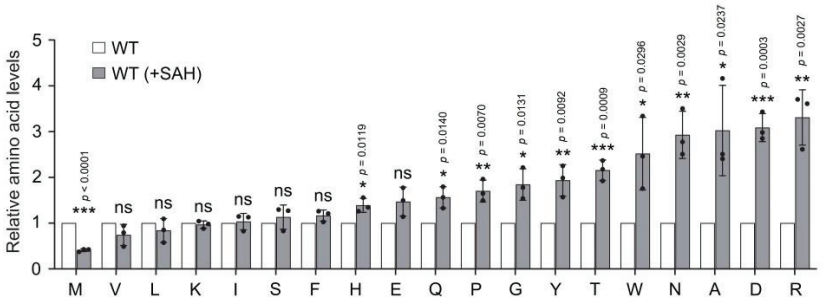
WT
WT (+SAH)
Relative amino acid levels
M V L K I S F H E Q P G Y T W N A D R

Fig. 7 Supplementation of SAH decreased intracellular methionine levels.

(A, B) Heat map (A) or volcano plot (B) showing metabolite levels in WT cells with or without SAH treatment. $n = 3$. FDR < 0.05, two-sided unpaired *t*-test. See also in Table 4. (C) Metabolite changes in the presence or absence of SAH in WT cells. Red and blue show increased and decreased metabolites, respectively. For a complete list, see Table 4. Mean±S.D. (n = 3). $^{*}p < 0.05$; $^{**}p < 0.01$; $^{***}p < 0.001$ (two-sided unpaired *t*-test assuming equal variance). (D) Values of amino acids in WT cells were set to one, respectively, after which the amino acids values when SAH was added were compared. Mean±S.D. (n = 3). $^{*}p < 0.05$; $^{**}p < 0.01$; $^{***}p < 0.001$ (two-sided unpaired *t*-test assuming equal variance).

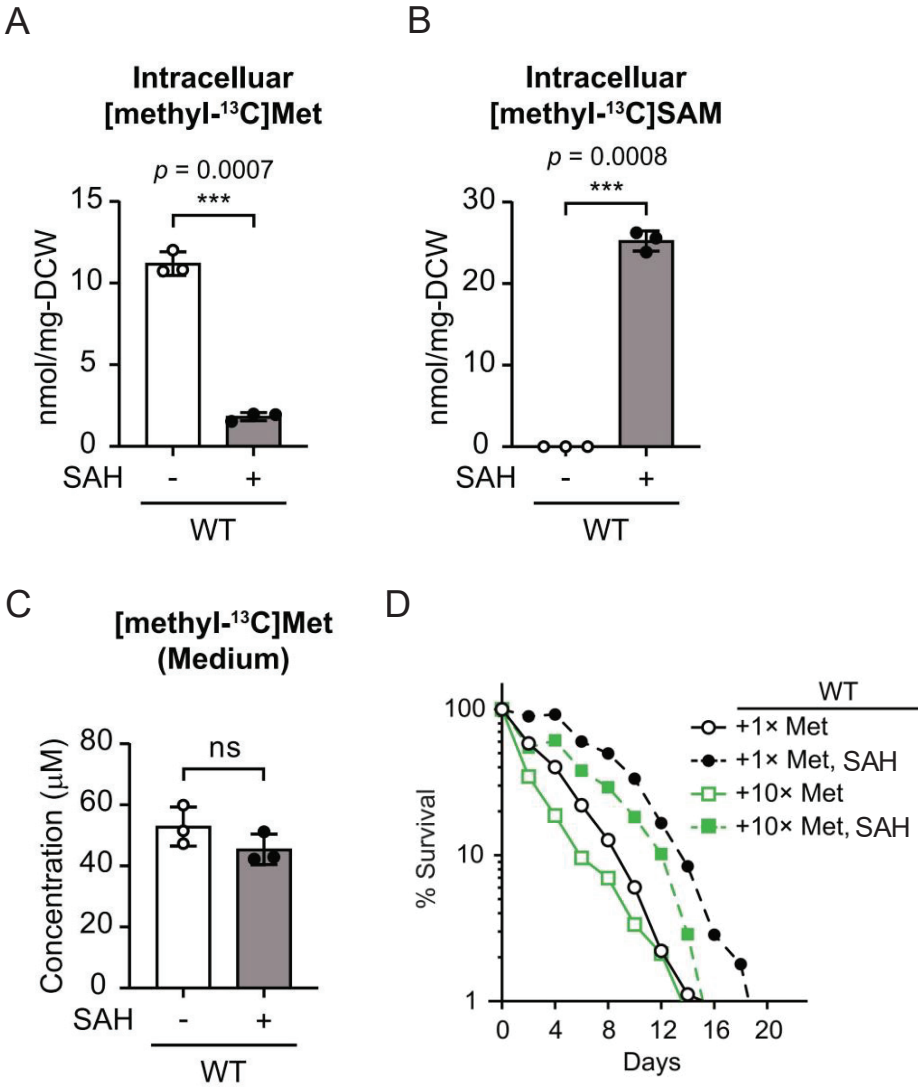

Fig. 8 SAH promoted SAM synthesis and consumes methionine.

(A-C) Intracellular [methyl-^{13}C]Met (A), Intracellular [methyl-^{13}C]SAM levels (B), and [methyl-^{13}C]Met levels in the medium (C) were assessed using CE-TOFMS. Mean ± S.D, $n = 3$, two-sided unpaired t-test. (D) The CLS curve is indicated. ns, not significant; ***$p < 0.001$. Statistical analyses are shown in Table 5.

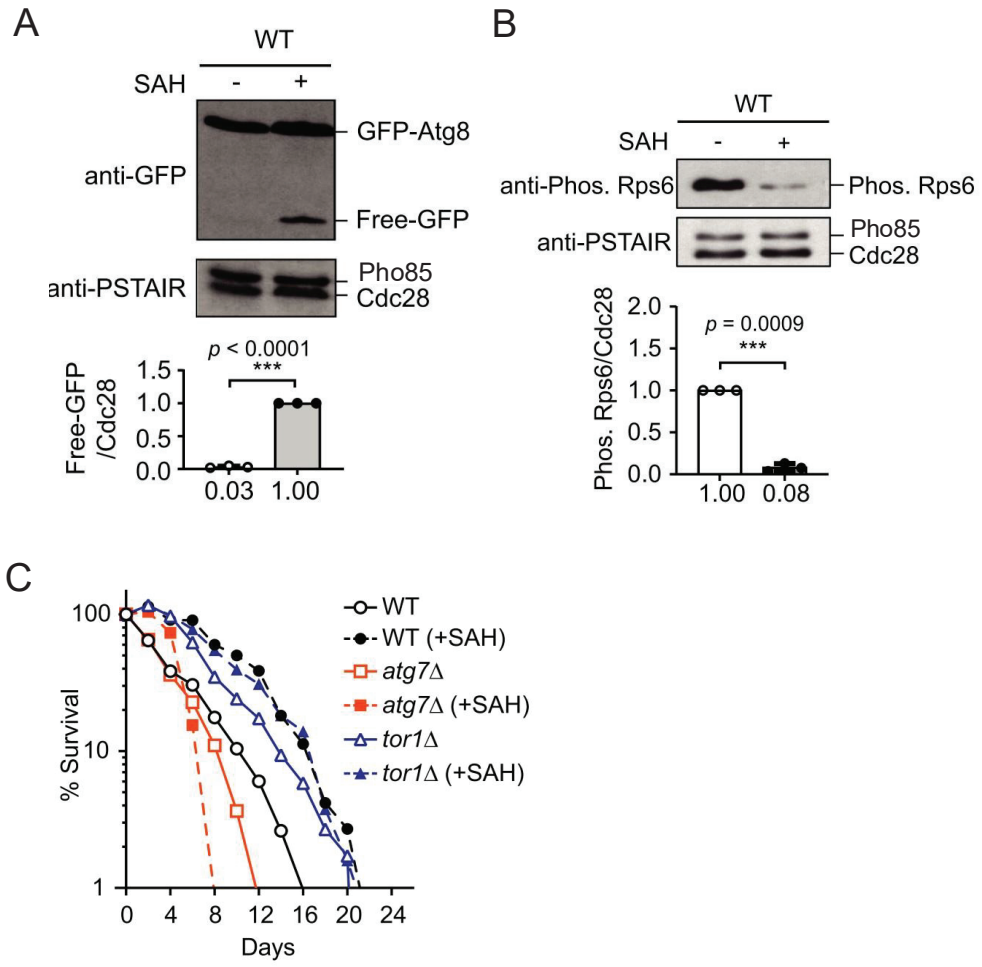

Fig. 9 SAH inhibits activity of mTORC1 and mimics the effects of MetR

(A, B) The relative intensity of free GFP (A) or phosphorylated Rps6 (B) normalized to Cdc28 is shown. Mean ± SD, $n = 3$, two-sided unpaired *t*-test. (C) The CLS curve is indicated. ns, not significant; ***$p < 0.001$. Statistical analyses are shown in Table 5.

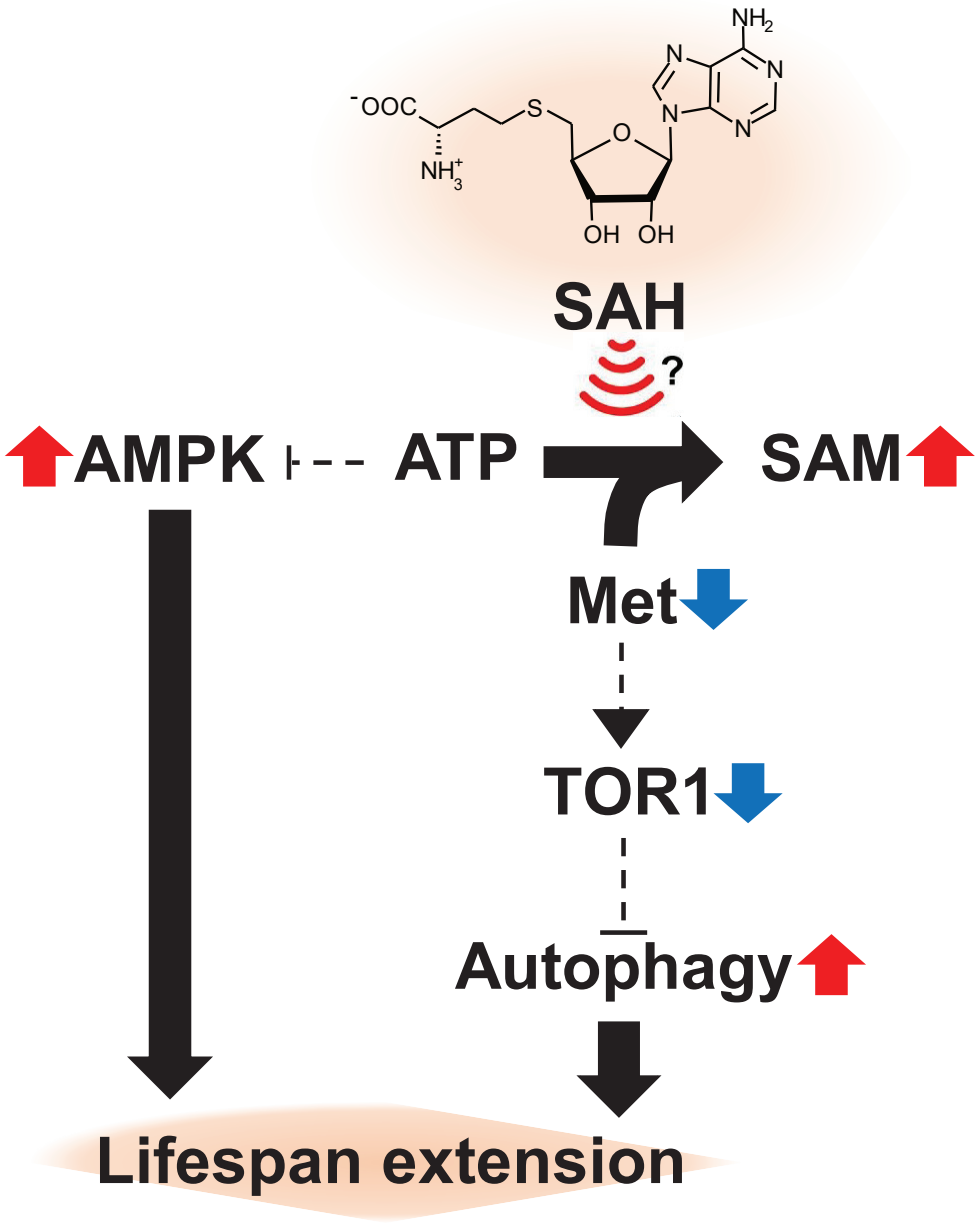

Fig. 10 SAH mimics MetR by promoting SAM synthesis

Table 3 Strains used in Chapter 2

Strain	**Name**	**Genotype**	**Source of Reference**
W303-1A	WT	*MATa* ; *trp1-1 leu2-3,112 ade2-1 ura3-1 his3-11,15 can1-100*	NBRP/YGRP
YMA32	*tor1* Δ	*MATa* ; *tor1* Δ*::kanMX4*	Lab. Stock
YYK1	*atg7* Δ	*MATa* ; *atg7* Δ*::kanMX4*	Lab. Stock

Table 4 Metabolomics data in SAH treated cells

						data_normarized					
	log2(Fold change)	-log10(*P* value)	Fold change	*P* value	FDR	WT 1	WT 2	WT 3	WT(+SAH) 1	WT(+SAH) 2	WT(+SAH) 3
Guanosine	4.7907	5.9647	27.679	**1.08E-06**	0.00016377	-0.9454516	-0.9454516	-0.8453805	0.89465614	0.89465614	0.94697149
SAM+	7.3231	5.3492	160.13	**4.47E-06**	0.00033784	-0.8464149	-1.0099067	-0.8775598	0.94710046	0.90494098	0.88183994
Ornithine	3.6684	4.8412	12.714	**1.44E-05**	0.00043265	-0.9447023	-1.0126553	-0.7727615	0.91809662	0.89392592	0.91809662
Inosine	5.5227	4.8066	45.973	**1.56E-05**	0.00043265	-0.771287	-1.0187021	-0.939784	0.90307676	0.92361959	0.90307676
Cystathionine	4.1186	4.7781	17.371	**1.67E-05**	0.00043265	-0.9381846	-1.0188779	-0.772416	0.89289433	0.89289433	0.94368982
Citrulline	-2.4238	4.7647	0.18636	**1.72E-05**	0.00043265	1.00819528	0.78295491	0.93818601	-0.921971	-0.9629105	-0.8444547
Guanine	2.551	4.5497	5.8602	**2.82E-05**	0.00060836	-0.8236466	-1.0640155	-0.8390674	0.84198596	0.92869786	0.95604562
Cytidine	2.1194	4.2633	4.3452	**5.45E-05**	0.0010295	-0.9455222	-1.0403249	-0.7362349	0.83954213	0.8919694	0.99057042
2-Isopropylmalate	1.4785	4.1366	2.7867	**7.30E-05**	0.0012249	-0.7002966	-1.047112	-0.9720761	0.94020304	0.91519444	0.86408718
5-Methylthioadenosine	7.526	4.0737	184.31	**8.44E-05**	0.0012742	-0.945459	-0.945459	-0.8271283	0.69707984	1.01048327	1.01048327
N-Acetylornithine	2.624	3.95	6.1644	**0.0001122**	0.0014823	-0.7759343	-1.0681986	-0.8707588	1.03639607	0.92831577	0.75017988
SAH	7.5757	3.9289	190.77	**0.0001178**	0.0014823	-1.0389927	-0.9905326	-0.6847823	1.00276017	0.86545189	0.84609554
Thr	1.1285	3.739	2.1864	**0.0001824**	0.0021185	-0.7286581	-1.1571636	-0.8225372	0.86538508	0.86538508	0.97758871
Citrate	2.3271	3.5343	5.0181	**0.0002922**	0.0031515	-0.9269233	-0.8082779	-0.9650996	0.63416968	0.93441771	1.13171339
GABA	0.5667	3.4465	1.4811	**0.0003577**	0.0036005	-0.683061	-0.8080745	-1.2050792	0.8697671	0.8697671	0.95668056
Arg	1.6919	3.4115	3.2308	**0.0003877**	0.0036592	-0.6676172	-1.1408752	-0.8859713	0.82900676	0.79037492	1.07508198
Uridine	1	3.3271	2	**0.0004709**	0.0040204	-0.7529439	-1.1840586	-0.7529439	0.71945529	0.93463735	1.03585384
Hypoxanthine	2.1155	3.3194	4.3333	**0.0004793**	0.0040204	-0.6183126	-1.1976303	-0.8735711	0.81868872	0.93541262	0.93541262
p-Aminobenzoate	-1.9809	3.2573	0.25333	**0.000553**	0.0043951	1.22104707	0.68696747	0.77784422	-0.9629443	-0.9629443	-0.7599701
N6,N6,N6-Trimethyllysine	1.7146	3.1954	3.2821	**0.0006378**	0.0044765	-0.8093181	-1.2095923	-0.6630376	0.94487484	0.72575795	1.01131528
5-Aminovalerate	1.5229	3.1947	2.8737	**0.0006387**	0.0044765	-0.8646027	-0.6654904	-1.1518118	0.66316479	1.06167283	0.95706721
5-Aminolevulinate	1.6189	3.1856	3.0714	**0.0006522**	0.0044765	-0.6701228	-1.1283631	-0.8828212	1.14485283	0.70770912	0.8287452
Adenosine	2.8842	3.1373	7.3832	**0.000729**	0.0047858	-1.1046169	-1.0117727	-0.5616269	0.78316526	0.82066973	1.07418154
Asn	1.5278	3.0777	2.8834	**0.0008361**	0.0052109	-0.596766	-1.2581052	-0.8188262	0.92700792	0.81968159	0.92700792
Dodecanedioate	0.70083	3.0599	1.6254	**0.0008712**	0.0052109	-1.0600074	-0.6728278	-0.9395112	1.05435025	0.56364597	1.05435025
3-Hydroxykynurenine	2.5471	3.0471	5.8444	**0.0008973**	0.0052109	-0.5757966	-1.0878963	-1.0076646	1.13360645	0.8016573	0.73609373
Pimelate	1.1424	3.0276	2.2075	**0.0009385**	0.0052484	-0.8420239	-0.7200405	-1.1077593	0.90240502	0.59285916	1.1745595
Sebacate	0.89997	2.9909	1.866	**0.0010211**	0.0055068	-0.6697905	-0.7858901	-1.2111642	0.89457451	0.66692757	1.10534278
Asp	1.6226	2.9053	3.0794	**0.0012437**	0.0063746	-1.0373683	-0.9558609	-0.6661435	0.62246233	0.78988508	1.24702526
Azelate	0.68093	2.8974	1.6032	**0.0012665**	0.0063746	-0.5370223	-1.060812	-1.060812	0.8159583	0.7006344	1.14205356
1-Methyladenosine	1.0204	2.865	2.0285	**0.0013647**	0.0064869	-0.4683803	-1.1371072	-1.0501012	0.88748961	1.01475815	0.75334097
Glutathione(ox)	1.5783	2.8618	2.9861	**0.0013747**	0.0064869	-0.9878812	-0.9165812	-0.75082	0.47765836	0.98620078	1.19142328
Glycolate	0.40911	2.6986	1.3279	**0.0020018**	0.0086661	-0.6728902	-0.6728902	-1.2921684	1.10717659	0.8821475	0.64862476
Ru5P	0.61891	2.698	1.5357	**0.0020046**	0.0086661	-0.8049033	-0.8049033	-1.028072	0.64553326	0.64553326	1.34681211
Met	-1.2592	2.6971	0.41778	**0.0020087**	0.0086661	1.14251098	0.60400314	0.89126095	-0.500149	-1.0865779	-1.0510481
Orotate	1.0135	2.6642	2.0188	**0.0021668**	0.0087921	-0.996459	-1.227863	-0.4095338	0.99139923	0.82122826	0.82122826
NADP+	0.95777	2.6508	1.9423	**0.0022347**	0.0087921	-1.2458063	-0.6218486	-0.7645613	0.67033515	0.75413725	1.20774373
Ala	1.5212	2.6452	2.8704	**0.0022636**	0.0087921	-0.5899183	-1.3721127	-0.6694962	0.95051962	0.8889643	0.79204338
Pyridoxamine 5'-phosphate	1.3663	2.6438	2.5781	**0.0022708**	0.0087921	-0.5191278	-1.3657465	-0.7464806	0.8771183	0.8771183	0.8771183
N-epsilon-Acetyllysine	0.83254	2.5757	1.7808	**0.0026565**	0.010028	-0.4706443	-1.2532388	-0.8986564	0.63916907	0.8801353	1.10323518
2AB	0.81399	2.4896	1.7581	**0.0032391**	0.011929	-0.3920006	-1.2699412	-0.9484048	1.01038932	0.67095349	0.92900378
N-Acetylglutamate	-1.1726	2.4269	0.44364	**0.0037422**	0.013454	0.59187672	0.84122363	1.16756091	-1.1281744	-1.069365	-0.4031218
Terephthalate	0.87832	2.3685	1.8382	**0.0042807**	0.015032	-0.9412101	-0.5754596	-1.0743106	0.38724044	0.94275247	1.26098739
Gly	0.85378	2.3201	1.8072	**0.0047853**	0.016422	-0.4137216	-1.4408484	-0.727869	0.86081299	0.86081299	0.86081299
Itaconate	0.82782	2.2737	1.775	**0.0053245**	0.017867	-1.4030865	-0.5513163	-0.6193845	0.98797067	0.55810165	1.02771494
beta-Ala-Lys	-0.76939	2.1146	0.58667	**0.007681**	0.025214	0.72404276	0.72404276	1.09214518	-1.4419112	-0.7447131	-0.3536064
Gln	0.61566	2.0963	1.5323	**0.0080116**	0.02574	-0.3159665	-1.4654461	-0.7545396	0.76405777	0.76405777	1.00783656
Adenine	4.2742	2.0085	19.35	**0.0098056**	0.030847	-0.2010551	-1.1388946	-1.174151	0.49914382	0.95902881	1.05592819
cis-Aconitate	0.71149	1.9121	1.6375	**0.012243**	0.037727	-0.1383384	-1.1397262	-1.2092625	0.70862516	0.62903292	1.14966903
NAD+	0.39366	1.8889	1.3137	**0.012916**	0.039006	-0.2438826	-1.5500181	-0.6864973	0.82724284	0.73742814	0.91572691
Orotidine 5'-monophosphate	-1.2433	1.8507	0.42241	**0.014101**	0.04175	0.37603668	0.87047242	1.22210105	-1.1999035	-1.0602445	-0.2084622
Pro	0.74351	1.8336	1.6742	**0.014669**	0.042597	-0.1389144	-1.402259	-0.9219577	1.1244303	0.71386473	0.62483606
N-Acetylhistidine	0.48321	1.7977	1.3978	**0.015934**	0.045397	-0.0682234	-1.4433415	-0.9397207	0.72518928	0.94499961	0.78109671
Succinate	0.6567	1.6988	1.5765	**0.02001**	0.055954	-0.1301146	-0.8023538	-1.4834369	1.1352409	0.76258414	0.51808027
gamma-Glu-2AB	1.1535	1.69	2.2245	**0.020419**	0.05606	0.0226032	-1.1417369	-1.2934185	0.5894707	0.99432371	0.82875772
ATP	2.1773	1.6383	4.5231	**0.023001**	0.061132	-1.0601654	-0.5695136	-0.7624263	0.35702981	1.63889645	0.39617906
Malate	0.69515	1.6353	1.619	**0.023158**	0.061132	0.06531456	-1.1218792	-1.3343312	0.70457084	0.98175416	0.70457084
Fumarate	0.71707	1.6275	1.6438	**0.02358**	0.061132	-0.3208296	-1.105762	-0.9610807	1.50060462	0.67312472	0.21394293
Adipate	0.59202	1.6219	1.5074	**0.023886**	0.061132	-0.0181722	-1.3243792	-1.0427958	1.16030416	0.43702897	0.7880141
2PG	0.96347	1.6022	1.95	**0.024991**	0.062894	-0.324054	-1.2280264	-0.8249978	0.09054658	1.34821271	0.93831898
Homoserine	1.6606	1.5312	3.1615	**0.029429**	0.072849	-0.8047759	-0.9503048	-0.5904171	-0.1369188	1.22221806	1.26019857
Malonate	0.63263	1.5199	1.5504	**0.030204**	0.073563	-1.2968155	-0.2868929	-0.756509	0.3193529	0.50066594	1.52019854
S-Lactoylglutathione	1.9795	1.4641	3.9437	**0.034348**	0.082307	-1.3653719	-0.4938797	-0.4537766	-0.002633	1.20671316	1.10894802
Tyr	0.90103	1.4574	1.8674	**0.034885**	0.082307	0.09649228	-1.4214988	-0.9846139	1.12170977	0.45836905	0.72954159
His	0.45638	1.4265	1.3721	**0.037452**	0.086928	0.08513291	-1.5515767	-0.8272154	1.07808432	0.60778742	0.60778742
Spermidine	0.71811	1.4203	1.645	**0.037995**	0.086928	-1.1059963	-0.078358	-1.1059963	1.32543457	0.07928547	0.88563055
UDP-N-acetylglucosamine	0.38219	1.3903	1.3033	**0.040709**	0.091748	0.20812273	-1.0671799	-1.4150739	0.7809758	0.95953094	0.53362436
Glu	0.52237	1.3792	1.4363	**0.041761**	0.092734	-0.1804353	-1.6029013	-0.4846466	0.36770749	0.61656995	1.28370586
2-Hydroxyglutarate	0.87898	1.3346	1.8391	**0.04628**	0.10128	-0.8198134	0.09824681	-1.5207864	0.2852093	0.91181682	1.04532681

Pelargonate	-0.48162	1.2825	0.71617	0.052175	0.11255	0.39404158	0.70444704	1.11211575	-1.6998952	-0.4693973	-0.0413119
Diethanolamine	-0.32591	1.2678	0.79779	0.053971	0.11478	0.48455911	0.33468141	1.38202782	-0.3865672	-1.5955314	-0.2191698
Glutarate	0.81979	1.2455	1.7652	0.056823	0.11917	-1.1574644	0.12819899	-1.1574644	0.32965324	0.44321392	1.41386263
UMP	-2.2395	1.2215	0.21176	0.060049	0.12421	0.2260572	0.75278723	1.19184341	-1.5135037	-0.8056035	0.14841937
Hexanoate	-0.32193	1.1858	0.8	0.065193	0.13303	0.42053999	0.64744692	1.07791089	-1.7719203	-0.3143381	-0.0596394
Decanoate	-0.60181	1.1679	0.65893	0.06794	0.13679	0.22650329	0.7893624	1.11716457	-1.6945758	-0.4535755	0.01512103
Cysteine-glutathione disulphide	1.816	1.1492	3.5211	0.070927	0.13925	-1.6117383	0.28469693	-0.7922603	0.36995398	0.98999124	0.75935647
Benzoate	0.56064	1.1487	1.4749	0.071011	0.13925	0.11853135	-0.7411439	-1.4963084	0.36447162	1.38997771	0.36447162
Anthranilate	-0.64299	1.0948	0.64038	0.080384	0.15561	0.80071719	0.63838309	0.63838309	-1.7624417	-0.5979522	0.28291056
UDP-glucose	2.1052	1.0552	4.3026	0.088067	0.16833	0.2180401	-1.3236711	-0.9394914	1.32818204	0.7435935	-0.0266531
CTP	1.6555	1.0492	3.1504	0.089294	0.16854	-0.2153863	-0.6155447	-1.2091417	0.76009649	1.56620988	-0.2862336
Octanoate	-0.35614	1.0363	0.78125	0.091986	0.17148	0.40787606	0.72099064	0.90023507	-1.8093849	-0.4303072	0.21059037
F6P	1.6215	1.0296	3.0769	0.093418	0.17203	0.0422336	-1.1313077	-0.9342527	1.48994763	0.75828922	-0.22491
Dodecanoate	-0.83149	0.91216	0.56195	0.12242	0.22271	0.24974431	0.62901708	1.03499562	-1.8437144	-0.2207811	0.15073853
Thymidine	0.38655	0.90134	1.3073	0.12551	0.22561	-1.5175795	0.09826974	-0.4834813	-0.2568416	1.24650045	0.91313221
Urocanate	0.27302	0.84509	1.2083	0.14286	0.25379	-0.3282854	-0.3282854	-1.1866816	1.11622808	-0.6024063	1.32943062
G6P	1.9826	0.82752	3.952	0.14876	0.2589	0.44474728	-1.043003	-1.2254888	1.30087571	0.69935476	-0.176486
ADP	0.92961	0.82633	1.9048	0.14917	0.2589	-1.5758022	-0.1882498	-0.0583478	-0.3277827	0.90345087	1.24673169
N-Acetylputrescine	0.44746	0.80944	1.3636	0.15508	0.26611	0.69526149	-1.3895145	-1.1089234	0.81410607	0.17496425	0.81410607
Undecanoate	-0.54889	0.79491	0.68354	0.16036	0.27207	0.10833313	0.68948677	0.98847279	-1.858636	-0.1621324	0.23447573
4-Oxopentanoate	-0.18521	0.74724	0.87952	0.17896	0.30025	0.73960959	1.69251831	-0.7035777	-0.3213947	-0.7035777	-0.7035777
NMN	-0.37109	0.73556	0.7732	0.18384	0.30309	1.33735766	-0.3380452	0.71451183	-1.4963525	-0.5112001	0.29372837
Ala-Ala	0.92658	0.73362	1.9008	0.18466	0.30309	-0.9251045	-0.3165438	-0.4697071	-0.7882392	1.05225066	1.44734393
UDP	-0.89984	0.69989	0.53595	0.19958	0.32404	-0.1361011	1.1066281	0.69687653	-1.7453351	-0.2941878	0.37211935
Heptanoate	-0.20811	0.67279	0.86567	0.21242	0.33974	0.11265683	0.44663415	1.07130776	-1.8396145	-0.2376184	0.44663415
Phosphorylcholine	-1.2924	0.67011	0.40828	0.21374	0.33974	-0.3389467	0.54385771	1.42196143	-1.2556507	-0.8645064	0.4932846
CMP	-1.0118	0.64386	0.49593	0.22706	0.35714	-0.2801039	0.57666398	1.29320437	-1.3459752	-0.8551263	0.61133694
Saccharopine	-0.37197	0.63831	0.77273	0.22998	0.35801	1.91140413	-0.2559475	-0.0737144	-0.2559475	-0.2559475	-1.0698472
Thiamine	0.51722	0.61818	1.4312	0.24089	0.37117	0.65215173	-1.8913425	-0.3129394	0.73348738	0.2942156	0.52442725
S7P	0.79718	0.59041	1.7377	0.2568	0.39065	-1.3353959	-0.8078427	0.6333594	0.12775232	-0.0807868	1.46291373
R5P	-0.43857	0.58719	0.73786	0.25871	0.39065	1.02686005	0.32977199	0.14824471	0.66105997	-1.8013663	-0.3645704
4-Acetylbutyrate	-0.75147	0.57716	0.594	0.26475	0.39582	-0.0312958	1.98574863	-0.465322	-0.6380802	-0.6126195	-0.2384311
Trp	1.004	0.56887	2.0056	0.26985	0.39949	0.76829931	-1.1914919	-1.0527683	1.36357008	0.14592563	-0.0335349
N-Acetylaspartate	0.52195	0.5549	1.4359	0.27868	0.40855	-1.0772362	0.35253563	-0.7286987	-0.7286987	1.46017071	0.72192718
GMP	-0.90046	0.53043	0.53571	0.29483	0.42807	-0.3343858	0.54529286	1.20187927	-1.5055409	-0.6152014	0.70795606
Citraconate	0.28876	0.50897	1.2216	0.30976	0.44547	-1.0299748	0.94060683	-1.2866149	-0.2403051	0.67568116	0.94060683
Val	-0.40276	0.47334	0.75641	0.33625	0.479	1.05600757	-0.3435895	0.59985642	0.92711067	-0.9782547	-1.2611305
Melatonin	0.2713	0.46561	1.2069	0.34229	0.48304	-1.4205698	0.69081787	-0.5682588	-0.5682588	0.69081787	1.17545167
Glycerophosphorylcholine	-0.56961	0.44597	0.6738	0.35812	0.49774	1.44242797	-1.1154669	0.9340597	-0.2520653	-0.1652617	-0.8436938
Butyrate	-0.23001	0.44455	0.85263	0.35929	0.49774	-0.1324241	0.69536916	0.69536916	-1.9222537	0.10845238	0.55548717
PEP	0.39803	0.42807	1.3177	0.37319	0.51229	-1.2362456	0.73087599	-0.7210021	-0.7210021	0.94456045	1.00281335
Urea	0.36565	0.36951	1.2885	0.42706	0.57931	-0.412749	-0.8551464	0.16168495	1.93170842	-0.412749	-0.412749
NADPH	-0.94111	0.36685	0.52083	0.42968	0.57931	-1.0922201	1.20643525	0.98626985	-1.161902	0.14676645	-0.0853495
Ser	0.15843	0.36047	1.1161	0.43605	0.58268	0.32019822	-1.1962181	-0.2106406	-0.9876648	0.65292857	1.42139668
GTP	1.0759	0.31239	2.1081	0.48709	0.64356	-0.9505611	0.104564	-0.1320313	-0.8606872	1.82402561	0.01468997
3PG	0.30008	0.30969	1.2312	0.49013	0.64356	-1.3893264	1.08205616	-0.6644033	-0.5135578	0.95568518	0.52954616
F1,6P	0.38995	0.29176	1.3103	0.51078	0.6649	1.05853379	-0.9936642	-0.9936642	0.62353262	1.0097727	-0.7045107
Argininosuccinate	-0.35364	0.28524	0.78261	0.51851	0.66919	1.94828122	-0.1179421	-0.9174578	-0.3008087	-0.4941303	-0.1179421
Glucosamine	1.1997	0.27893	2.2969	0.52611	0.67174	0.95778382	-0.7425824	-1.1125186	1.38698954	0.10864252	-0.5983149
5-Oxoproline	1.1509	0.27623	2.2206	0.52938	0.67174	-1.1976162	0.12249969	0.18449234	-1.163337	0.86275412	1.19120704
Thiamine monophosphate	0.10257	0.24368	1.0737	0.57059	0.71799	0.92924958	-1.3730446	-0.3635932	-0.8509034	0.92924958	0.72904208
Glutathione(red)	1.7351	0.23876	3.329	0.57709	0.72016	0.83318545	-1.2223369	-0.4052633	1.53784655	-0.4271179	-0.3163139
Phe	0.1964	0.21812	1.1458	0.60518	0.74904	0.89300445	-1.2594398	-0.3723223	1.48340239	-0.3723223	-0.3723223
Phthalate	0.27922	0.21409	1.2135	0.61082	0.74987	-1.449386	0.49439234	0.22732554	-1.0151636	0.70726477	1.03556696
Methionine sulfoxide	-0.20231	0.2093	0.86916	0.61759	0.75206	1.17174558	-0.1887138	-0.2686388	1.25468734	-0.9281767	-1.0409036
UTP	-0.12114	0.2023	0.91946	0.62763	0.75237	0.53850642	0.53850642	-0.3822559	-1.2697671	1.40470589	-0.8296957
Glu-Glu	0.1822	0.19936	1.1346	0.63189	0.75237	-0.5683944	-0.5683944	0.45034827	-1.1779681	0.21616529	1.64824327
Acetyl CoA	0.40968	0.19874	1.3284	0.63279	0.75237	0.99819167	0.00145475	-0.3149536	1.34401403	-0.8725508	-1.1561561
Leu	-0.17333	0.1924	0.88679	0.64209	0.75747	1.09575112	-0.4480492	0.01890605	1.28471627	-0.8275155	-1.1238088
CDP	0.24602	0.18437	1.1859	0.65408	0.76563	-1.4399725	0.55885095	0.23773289	-1.0164474	0.55885095	1.1009851
Pyridoxine	0.66921	0.1657	1.5902	0.68282	0.79312	1.02235344	-0.6973163	-0.9131728	1.40747935	-0.0109246	-0.808419
Glycerate	-0.14018	0.15377	0.90741	0.70182	0.80897	-1.459849	0.69227394	1.31944283	-0.7251912	-0.1454433	0.31876675
GDP	-0.29852	0.14036	0.81308	0.72384	0.82802	-1.1355999	0.8989507	0.74675273	-1.3859073	0.58003873	0.29576502
N-Acetylglucosamine	-0.055495	0.11757	0.96226	0.76284	0.86608	-0.1157129	1.01162065	-0.4592123	1.34190278	-0.4592123	-1.3193859
NADH	-0.23704	0.10114	0.84848	0.79224	0.88123	0.9378494	-1.4939174	0.9378494	-0.3111371	0.63913546	-0.7097797
Nicotinamide	0.32563	0.10067	1.2532	0.7931	0.88123	-1.4483354	0.56459029	0.50355214	-1.1053352	0.69359713	0.79193104
Propionate	-0.033683	0.10035	0.97692	0.79369	0.88123	-0.2192732	0.50403136	0.09433155	-1.8785067	0.61543202	0.8839849
Choline	0.26849	0.085439	1.2045	0.82141	0.89879	0.37557798	-1.2351234	0.53192552	-0.5071059	-0.6882877	1.52301353
Pyruvate	-0.13058	0.078208	0.91346	0.8352	0.90731	1.40977941	-1.5378783	0.43019951	0.43019951	-0.2984099	-0.4338903
Lys	-0.025091	0.070786	0.98276	0.8496	0.91537	0.57849919	-1.5078128	1.20483549	0.57849919	-0.7740504	-0.0799707
Putrescine(1,4-Butanediamine)	-0.054448	0.068162	0.96296	0.85475	0.91537	1.46822821	-0.6320606	-1.1021964	0.86077651	-0.6924496	0.09770191
DHAP	-0.057144	0.064906	0.96117	0.86118	0.91576	1.37539442	-0.9556903	-0.6738842	1.11827011	-0.1902057	-0.6738842
Lactate	0.017487	0.059301	1.0122	0.87237	0.91621	-0.3101928	1.26604813	-1.1894463	0.635826	-1.038061	0.635826
Pentanoate	-0.026089	0.058311	0.98208	0.87436	0.91621	-0.7445308	0.95631523	0.01814595	-1.5710486	0.38480299	0.95631523
Uracil	0.34702	0.055613	1.2719	0.87981	0.91621	0.88949571	-0.6583034	-0.4511073	1.55440287	-0.3030057	-1.0314822
3-Methylbutanoate	0.0081279	0.033935	1.0056	0.92484	0.94863	-0.7426475	0.59561086	0.28437976	-1.6801133	0.77138508	0.77138508
Indole-3-ethanol	-0.22239	0.031617	0.85714	0.92979	0.94863	-1.4842811	1.14628318	0.46628252	-0.8868865	0.07009301	0.68850888
Glycerophosphate	-0.082953	0.019831	0.94412	0.95536	0.9665	1.07445868	-1.8063638	0.6503887	-0.0266799	-0.2225044	0.33070071
Ile	0.024662	0.0050904	1.0172	0.98835	0.98835	1.04901089	-0.9355749	-0.1347111	1.4075012	-0.5138679	-0.8723582

Table 5 *P* value for CLS analysis in Chapter 2

Figure	**Strain A**	**Strain B**	***P*-value against B**
8D	WT, 1×Met	WT, 10×Met	**<0.001**
	WT, 1×Met	WT, 1×Met, SAH	**<0.001**
	WT, 10×Met	WT, 10×Met, SAH	**<0.001**
	WT, 1×Met, SAH	WT, 10×Met, SAH	**<0.001**
9C	WT	WT, SAH	**<0.0001**
	tor1 Δ	*tor1* Δ	**<0.0001**
	WT, AdoHcy	*tor1* Δ, SAH	0.6151
	atg7 Δ	*atg7* Δ, SAH	**0.0134**

General conclusions

Aging is a universal phenomenon common to all organisms (López-Otín *et al*., 2016), and it is the result of a complex interplay and accumulation of various factors such as genomic instability, telomere attrition, loss of proteostasis, deregulated metabolic signals, mitochondrial dysfunction, and senescence of the immune system (de Cabo *et al*., 2014; López-Otín *et al*., 2016; Campisi *et al*., 2019). Thus, although aging is a complex process, studies of aging and lifespan have been conducted using various model organisms and it has become clear that similar to other life phenomena, aging and lifespan exhibit common mechanisms at the genetic level (Kenyon, 2005, 2010; Fontana *et al.*, 2010).

Some lifespan pathways discovered from yeast are highly conserved in higher organisms. For instance, CR is known to extend the lifespan of many model organisms, and the molecules involved in CR were first discovered in yeast studies. The effect of lowering the glucose concentration in yeast from 2% to 0.5% in the medium on lifespan extension of CR was found to depend on a sirtuin gene, Sir2 (Imai *et al*., 2000). Deletion of Sir2 did not result in CR-induced lifespan extension, which was also observed for the sirtuin gene in *C. elegans* and *Drosophila* (Tissenbaum and Guarente, 2001; Rogina and Helfand, 2004). In addition, Powers *et al*. (2006) screened about 4800 essential genes in budding yeast for identifying factors that extend lifespan and detected many mutations in the mTORC1 pathway. Moreover, they found that adding rapamycin, an inhibitor of mTORC1, extended lifespan. The mTORC1 pathway regulates important functions, such as protein synthesis and autophagy, which degrades and recycles proteins in the cell (Shimobayashi and Hall, 2014). Therefore, suppression of mTORC1 is critical for

lifespan extension by inhibiting protein translation and promoting autophagy. Thus, starting with yeast research, many pathways and molecular mechanisms that extend lifespan have been identified so far; however, the detailed mechanisms remain unclear. It has also become clear that several drugs and metabolites targeting mTORC1 extend lifespan (Chin, *et al*., 2014; Hine, *et al*., 2015); however, the relationship between their metabolic pathways and regulation of lifespan is not fully understood. In this study, the related factors in the Ca^{2+} signaling pathway were predicted to regulate lifespan as related to CR. Therefore, to search for a novel mechanism of lifespan extension in budding yeast, I analyzed lifespan extension involving Sko1, a downstream factor of the HOG pathway, and SAH, one of the Met metabolites.

In Chapter 1, I showed that Sko1 function, a regulator of the HOG pathway, suppressed the oxidative stress sensitivity and short lifespan of *hog1*Δ cells, indicating glycerol synthesis system-dependent resistance to oxidative stress and lifespan extension. Currently, abnormal or inappropriate function of MAPK pathway has been identified in a variety of diseases, such as cancer, inflammatory diseases, and diabetes (Kim and Choi, 2010). Hence, the lifespan regulation mechanisms involving the HOG pathway and its downstream target genes identified in this study are expected to lead to the discovery of new therapeutic agents and understanding of diseases using the stress-responsive MAPK pathway, which is homologous to the HOG pathway in higher organisms. Furthermore, yeast cells are exposed to osmotic, oxidative, and ethanol stresses during ethanol fermentation, and the results of this study analyzing the relationship between stress response pathways and survival during aging are expected to be applied to breeding yeast for fermentation.

In Chapter 2, I analyzed the mechanism of how the addition of SAH, a Met

metabolite, prolongs lifespan. I showed that SAH promotes SAM synthesis and consumes Met, thereby decreasing intracellular Met concentrations, via metabolomic analysis and L-[methyl-^{13}C]Met tracking. Furthermore, SAH inhibited TORC1 and activated autophagy, which was expected to mimic the effects of MetR. Met metabolism regulates a variety of metabolic processes, such as translation rates, gene expression, mitochondrial function, and autophagy. MetR can extend lifespan and delay the onset of aging-associated pathologies in most model organisms. Although genetic manipulation of Met metabolism and drug therapies such as metformin have been used as methods of MetR, it is not easy for us to try these methods. This study and Ogawa *et al*. (2022) showed that the metabolite of organism SAH mimics MetR in both yeast and nematodes, which may lead to safer and more effective lifespan extension. It is expected that a similar effect of MetR by SAH will be observed in further higher organisms in the future. In addition, more detailed analyses of the effect of SAH treatment on lifespan extension are expected to provide novel insights into the mechanisms of lifespan regulation by MetR.

Initially, both Sko1 and SAH were expected to control lifespan via CR. Indeed, promotion of glycerol synthesis, which activates Sir2, a component of CR, was essential for prolonging the lifespan of *sko1*Δ cells. Also, supplementation with SAH increased NAD^+, a component of CR, and spermidine, a natural polyamine that mimics CR. However, it is not well understood how these factors mediate lifespan extension via Sko1 deficiency and SAH. Therefore, exploring the specific factors of CR that are involved in these life span extensions is a challenge for future analysis.

In this study, I suggest two novel mechanisms of lifespan extension in budding yeast, and both of these mechanisms are expected to be highly conserved to other organisms, including humans. Therefore, I expect that our findings of the molecular

mechanisms that regulate lifespan in budding yeast will be applied to human health, aging and lifespan, and treatment of diseases.

Acknowledgements

First of all, I would like to express my great thanks to Professor Masaki Mizunuma for his constant guidance, not only in technical matters, but also in the way of being a researcher and its aspirations.

I have been greatly indebted to Professor Dai Hirata, Associate Professor Kazunori Kume, Assistant Professor Makoto Horikawa, Dr. Takafumi Ogawa for their constant discussion, guidance, and encouragement.

I am grateful to thank for Professor Masaki Mizunuma, Professor Seiji Kawamoto, Associate Professor Koichi Funato, Associate Professor Kazunori Kume for fruitful discussion and carefully reviewing this study.

I am deeply grateful to Professor T. Keith Blackwell, Professor Yoshikazu Oya, Professor Tomoyoshi Soga, Dr. Muneyoshi Kanai, Dr. Takafumi Ogawa, Eri Sanda, Kumiko Yonekita, Sachi Matsukami, Yuki Kohara for their technical guidance, discussions, and several experiments.

I also thanks *Mizunuma's Laboratory 2017-2023*, Takako Ezaki, Dr. Takafumi Ogawa, Yuto Takeuchi, Kenji Nishikawa, Haruka Kondo, Yuika Seo, Mayuka Tanetani, Sachi Matsukami, Saki Ueda, Konami Kawata, Yusaku Nakagaki, Maiko Baba, Chiho Funaki, Kana Watanabe, Matthew Spence, Miyuki Aohara, Syunya Takeo, Yuki Chikaishi, Takuya Tsuji, Kei Yoneda, Yuki Kohara, Takahiro Fujimoto, Sota Kanda, Kota Takashima, Sara Mizogami, Hiroya Matsuzaki, Mayu Tsutsumi, Harumi Hiramatsu, Rikuto Furuyama, Hiiro Yamashita for their constant guidance, support and help.

I have been a recipient of Japan Society for the Promotion of Science Fellowship (DC1) from April 2020 to March 2023, which I appreciate very much.

Finally, I would like to thank my parents and family from the bottom of my heart for their respect and support of my choice and decision.

References

Ables, G.P.; Johnson, J.E. Pleiotropic responses to methionine restriction. *Exp Gerontol*. 2017, 94, 83-88.

Annibal, A.; Tharyan, R.G.; Schonewolff, M.F.; Tam, H.; Latza, C.; Auler, M.M.K.; Grönke, S.; Partridge, L.; Antebi, A. Regulation of the one carbon folate cycle as a shared metabolic signature of longevity. *Nat. Commun.* 2021, 12, 3486.

Aramburu, J.; Rao, A.; Klee, C.B. Calcineurin: from structure to function. *Curr. Top Cell Regul*. 2000, 36, 237-295.

Bonkowski, M.S.; Sinclair, D.A. Slowing ageing by design: the rise of NAD^+ and sirtuin-activating compounds. *Nat. Rev. Mol. Cell Biol*. 2016, 17, 679-690.

Botstein, D.; Fink, G.R. Yeast: an experimental organism for 21st Century biology. *Genetics* 2011, 189, 695-704.

Campisi, J.; Kapahi, P.; Lithgow, G.J.; Melov, S.; Newman, J.C.; Verdin, E. From discoveries in ageing research to therapeutics for healthy ageing. *Nature* 2019, 571, 183-192.

Chin, R.M.; Fu, X.; Pai, M.Y.; Vergnes, L.; Hwang, H.; Deng, G.; Diep, S.; Lomenick, B.; Meli, V.S.; Monsalve, G.C.; *et al*. The metabolite α-ketoglutarate extends lifespan by inhibiting ATP synthase and TOR. *Nature* 2014, 510, 397-401.

Christopher, S.A.; Melnyk, S.; James, S.J.; Kruger, W.D. *S*-adenosylhomocysteine, but not homocysteine, is toxic to yeast lacking cystathionine beta-synthase. *Mol. Genet. Metab.* 2002, 75, 335–343.

de Cabo, R.; Carmona-Gutierrez, D.; Bernier, M.; Hall, M.N.; Madeo, F. The search for antiaging interventions: from elixirs to fasting regimens. *Cell* 2014, 157, 1515-1526.

Eisenberg, T.; Knauer, H.; Schauer, A.; Büttner, S.; Ruckenstuhl, C.; Carmona-Gutierrez, D.; Ring, J.; Schroeder, S.; Magnes, C.; Antonacci, L.; *et al*. Induction of autophagy by spermidine promotes longevity. *Nat. Cell Biol.* 2009, 11, 1305-1314.

Fabrizio, P.; Longo, V.D.; The chronological life span of *Saccharomyces cerevisiae*. *Aging Cell* 2007, 2, 73-81

Fontana, L.; Partridge, L.; Longo, V.D. Extending health life span-from yeast to humans. *Science* 2010, 328, 321-326

Hedbacker, K.; Carlson, M. SNF1/AMPK pathways in yeast. *Front Biosci*. 2008, 13, 2408-2420.

Hepowit, N.L.; Macedo, J.K.A.; Young, L.E.A.; Liu, K.; Sun, R.C.; MacGurn, J.A; Dickson, R.C. Enhancing lifespan of budding yeast by pharmacological lowering of amino acid pools. *Aging (Albany NY)* 2021, 13, 7846-7871.

Hine, C.; Harputlugil, E.; Zhang, Y.; Ruckenstuhl, C.; Lee, B.C.; Brace, L.; Longchamp, A.; Treviño-Villarreal, J.H.; Mejia, P.; Ozaki, C.K.; *et al*., Endogenous hydrogen sulfide production is essential for dietary restriction benefits. *Cell* 2015, 160, 132-144.

Howitz, K.T.; Bitterman, K.J.; Cohen, H.Y.; Lamming, D.W.; Lavu, S.; Wood, J.G.; Zipkin, R.E.; Chung, P.; Kisielewski, A.; Zhang, L.L.; *et al.* Small molecule activators of sirtuins extend *Saccharomyces cerevisiae* lifespan. *Nature* 2003, 425, 191-196.

Imai, S.; Armstrong, C.M.; Kaeberlein, M.; Guarente, L. Transcriptional silencing and longevity protein Sir2 is an NAD-dependent histone deacetylase. *Nature* 2000, 403, 795-800.

Johnson, J.E.; Johnson, F.B. Methionine restriction activates the retrograde response and confers both stress tolerance and lifespan extension to yeast, mouse and human cells. *PLoS One* 2014, 9, e97729.

Kaeberlein, M.; Andalis, A.A.; Fink, G.R.; Guarente, L. High osmolarity extends life span in *Saccharomyces cerevisiae* by a mechanism related to calorie restriction. *Mol. Cell. Biol.* 2002, 22, 8056-8066.

Kaeberlein, M.; McVey, M.; Guarente, L. The *SIR2/3/4* complex and *SIR2* alone promote longevity in *Saccharomyces cerevisiae* by two different mechanisms. *Genes Dev*. 1999, 13, 2570-2580.

Kenyon, C. The plasticity of aging: insights from long-lived mutants. *Cell* 2005, 120, 449-460.

Kenyon, C., J. The genetics of ageing. *Nature* 2010, 464, 504-512.

Kim, E.K.; Choi, E.J. Pathological roles of MAPK signaling pathways in human diseases. *Biochim. Biophys. Acta.* 2010, 1802, 396-405.

Kobayashi, Y.; Inai, T.; Mizunuma, M.; Okada, I.; Shitamukai, A.; Hirata, D.; Miyakawa, T. Identification of Tup1 and Cyc8 mutations defective in the responses to osmotic stress. *Biochem. Biophys. Res. Commun.* 2008, 68, 50-55.

Longtine, M.S.; McKenzie, A. 3rd.; Demarini, D.J.; Shah, N.G.; Wach, A.; Brachat, A.; Philippsen, P.; Pringle, J.R. Additional modules for versatile and economical PCR-based gene deletion and modification in *Saccharomyces cerevisiae*. *Yeast* 1998, 14, 953-961.

López-Otín, C.; Galluzzi, L.; Freije, J.M.P.; Madeo, F.; Kroemer, G. Metabolic Control of Longevity. *Cell* 2016, 166, 802-821.

Mair, W.; Dillin, A. Aging and survival: the genetics of life span extension by dietary restriction. *Annu. Rev. Biochem.* 2008, 77, 727-754

Miller, R.A.; Buehner, G.; Chang, Y.; Harper, J.M.; Sigler, R.; Smith-Wheelock, M. Methionine-deficient diet extends mouse lifespan, slows immune and lens aging, alters

glucose, T4, IGF-I and insulin levels, and increases hepatocyte MIF levels and stress resistance. *Aging Cell* 2005, 4, 119-125

Ministry of Health, Labor and Welfare. https://www.mhlw.go.jp/stf/newpage_21481.html, accessed on 18 Dec 2022b.

Ministry of Health, Labor and Welfare.
https://www.mhlw.go.jp/toukei/saikin/hw/life/life21/dl/life18-02.pdf,
accessed on 18 Dec 2022a

Mizunuma, M.; Hirata, D.; Miyahara, K.; Tsuchiya, E.; Miyakawa, T. Role of calcineurin and Mpk1 in regulating the onset of mitosis in budding yeast. *Nature* 1998, 392, 303-306.

Mizunuma, M.; Hirata, D.; Miyaoka, R.; Miyakawa, T. GSK-3 kinase Mck1 and calcineurin coordinately mediate Hsl1 down-regulation by Ca^{2+} in budding yeast. *EMBO J*. 2001, 20, 1074-1085.

Mizunuma, M.; Miyamura, K.; Hirata, D.; Yokoyama. H.; Miyakawa, T. Involvement of *S*-adenosylmethionine in G1 cell-cycle regulation in *Saccharomyces cerevisiae*. *Proc. Natl. Acad. Sci. U S A.* 2004, 101, 6086-6091.

Mizunuma, M.; Tsubakiyama, R.; Ogawa, T.; Shitamukai, A.; Kobayashi, Y.; Inai, T.; Kume, K.; Hirata, D. Ras/cAMP-dependent protein kinase (PKA) regulates multiple aspects of cellular events by phosphorylating the Whi3 cell cycle regulator in budding yeast. *J. Biol. Chem.* 2013, 288, 10558-10566.

Mortimer, R.K.; Johnston J.R. Life span of individual yeast cells. *Nature* 1959, 183, 1751-1752.

Nair, U.; Thumm, M.; Klionsky, D.J.; Krick, R. GFP-Atg8 protease protection as a tool to monitor autophagosome biogenesis. *Autophagy* 2011, 7, 1546-1550.

Obata, F; Miura, M. Enhancing *S*-adenosyl-methionine catabolism extends *Drosophila* lifespan. *Nat. Commun.* 2015, 6, 8332.

Ogawa, T.; Masumura, K.; Kohara, Y.; Kanai, M.; Soga, T.; Ohya, Y.; Blackwell, T.K.; Mizunuma, M.; *S*-adenosyl-L-homocysteine extends lifespan through methionine restriction effects. *Aging Cell* 2022, 21, e13604.

Ogawa, T.; Tsubakiyama, R.; Kanai, M.; Koyama, T.; Fujii, T.; Iefuji, H.; Soga, T.; Kume, K.; Miyakawa, T.; Hirata, D.; Mizunuma, M. Stimulating *S*-adenosyl-l-methionine synthesis extends lifespan via activation of AMPK. *Proc. Natl. Acad. Sci. U S A.* 2016, 113, 11913-11918.

Orentreich, N.; Matias, J.R.; Defelice, A.; Zimmerman, J.A. Low methionine ingestion by rats extends life span. *J. Nutr.* 1993, 123, 269-274.

Pang, Z.; Chong, J.; Zhou, G.; de Lima Morais, D.A.; Chang, L.; Barrette, M.; Gauthier, C.; Jacques, P.É.; Li, S.; Xia, J. MetaboAnalyst 5.0: narrowing the gap between raw spectra and functional insights. *Nucleic Acids Res*. 2021, 49, W388-W396.

Parkhitko, A.A.; Jouandin, P.; Mohr, S.E.; Perrimon, N. Methionine metabolism and methyltransferases in the regulation of aging and lifespan extension across species. *Aging Cell* 2019, 18, e13034.

Plummer, J.D.; Johnson, J.E. Extension of Cellular Lifespan by Methionine Restriction Involves Alterations in Central Carbon Metabolism and Is Mitophagy-Dependent. *Front. Cell Dev. Biol.* 2019, 7,301.

Powers, R.W. 3rd.; Kaeberlein, M.; Caldwell, S.D.; Kennedy, B.K.; Fields, S. Extension of chronological life span in yeast by decreased TOR pathway signaling. *Genes Dev.* 2006, 20, 174-184.

Proft, M.; Struhl, K. Hog1 kinase converts the Sko1-Cyc8-Tup1 repressor complex into

an activator that recruits SAGA and SWI/SNF in response to osmotic stress. *Mol. Cell* 2002 ,9, 1307-1317.

Rep, M.; Proft, M.; Remize, F.; Tamás, M.; Serrano, R.; Thevelein, J.M.; Hohmann, S. The *Saccharomyces cerevisiae* Sko1p transcription factor mediates HOG pathway-dependent osmotic regulation of a set of genes encoding enzymes implicated in protection from oxidative damage. *Mol. Microbiol.* 2001, 40, 1067-1083.

Rogina, B.; Helfand, S.L. Sir2 mediates longevity in the fly through a pathway related to calorie restriction. *Proc. Natl. Acad. Sci. U S A*. 2004, 101, 15998-16003.

Ruckenstuhl, C.; Netzberger, C.; Entfellner, I.; Carmona-Gutierrez, D.; Kickenweiz, T.; Stekovic, S.; Gleixner, C.; Schmid, C.; Klug, L.; Sorgo, A.G.; *et al*. Lifespan extension by methionine restriction requires autophagy-dependent vacuolar acidification. *PLoS Genet*. 2014, 10, e1004347.

Saito, H.; Posas, F. Response to hyperosmotic stress. *Genetics* 2012, 192, 289-318.

Satoh, K.; Yachida, S.; Sugimoto, M.; Oshima, M.; Nakagawa, T.; Akamoto, S.; Tabata, S.; Saitoh, K.; Kato, K.; Sato, S.; *et al*. Global metabolic reprogramming of colorectal cancer occurs at adenoma stage and is induced by MYC. *Proc. Natl. Acad. Sci. U S A*. 2017, 114, E7697-E7706.

Shimobayashi, M.; Hall, M.N. Making new contacts: the mTOR network in metabolism and signalling crosstalk. *Nat. Rev. Mol. Cell Biol.* 2014, 15, 155-162.

Sinclair, D.A.; Guarente, L. Extrachromosomal rDNA circles--a cause of aging in yeast. *Cell* 1997, 91, 1033-1042.

Smith, D.L.Jr.; McClure, J.M.; Matecic, M.; Smith, J.S. Calorie restriction extends the chronological lifespan of *Saccharomyces cerevisiae* independently of the Sirtuins. *Aging Cell* 2007, 6, 649-662.

Soga, T.; Baran, R.; Suematsu, M.; Ueno, Y.; Ikeda, S.; Sakurakawa, T.; Kakazu, Y.; Ishikawa, T.; Robert, M.; Nishioka, T.; Tomita, M. Differential metabolomics reveals ophthalmic acid as an oxidative stress biomarker indicating hepatic glutathione consumption. *J. Biol. Chem.* 2006, 281, 16768-16776.

Soga, T.; Igarashi, K.; Ito, C.; Mizobuchi, K, Zimmermann HP, Tomita M. Metabolomic profiling of anionic metabolites by capillary electrophoresis mass spectrometry. *Anal Chem.* 2009, 81, 6165-6174.

Soga, T.; Ohashddi, Y.; Ueno, Y.; Naraoka, H.; Tomita, M.; Nishioka, T. Quantitative metabolome analysis using capillary electrophoresis mass spectrometry. *J. Proteome Res*. 2003, 2, 488-494.

Sutphin, G.L.; Kaeberlein, M. Dietary restriction by bacterial deprivation increases life span in wild-derived nematodes. *Exp. Gerontol.* 2008, 433, 130-135.

Thomas, D.; Surdin-Kerjan, Y.; Metabolism of sulfur amino acids in *Saccharomyces cerevisiae*. *Microbiol. Mol. Biol. Rev*. 1997, 61, 503-532.

Tissenbaum, H.A.; Guarente, L. Increased dosage of a *sir-2* gene extends lifespan in *Caenorhabditis elegans*. *Nature*. 2001, 410, 227-230.

Tsubakiyama, R.; Mizunuma, M.; Gengyo, A.; Yamamoto, J.; Kume, K.; Miyakawa, T.; Hirata, D. Implication of Ca^{2+} in the regulation of replicative life span of budding yeast. *J. Biol. Chem.* 2011, 286, 28681-28687.

Wood, J. G.; Rogina, B.; Lavu, S.; Howitz, K.; Helfand, S. L.; Tatar, M.; Sinclair, D. Sirtuin activators mimic caloric restriction and delay ageing in metazoans. *Nature* 2004, 430, 686–689.

Wu, Z.; Song, L.; Liu, S.Q.; Huang, D. Independent and additive effects of glutamic acid and methionine on yeast longevity. *PLoS One*, 2013, 8, e79319.

Wullschleger, S.; Loewith, R.; Hall, M.N. TOR signaling in growth and metabolism. *Cell* 2006, 124, 471-484

Yamamoto, K.; Tatebayashi, K.; Tanaka, K.; Saito, H. Dynamic control of yeast MAP kinase network by induced association and dissociation between the Ste50 scaffold and the Opy2 membrane anchor. *Mol. Cell* 2010, 40, 87-98.

Zou, K.; Rouskin, S.; Dervishi, K.; McCormick, M.A.; Sasikumar, A.; Deng, C.; Chen, Z.; Kaeberlein, M.; Brem, R.B.; Polymenis, M.; *et al*. Life span extension by glucose restriction is abrogated by methionine supplementation: Cross-talk between glucose and methionine and implication of methionine as a key regulator of life span. *Sci. Adv.* 2020, 6, eaba1306.